

# $\gamma\delta$ T cells provide the early source of IFN- $\gamma$ to aggravate lesions in spinal cord injury

Guodong Sun,<sup>1\*</sup> Shuxian Yang,<sup>1\*</sup> Guangchao Cao,<sup>1\*</sup> Qianghua Wang,<sup>2</sup> Jianlei Hao,<sup>1</sup> Qiong Wen,<sup>1</sup> Zhizhong Li,<sup>3</sup> Kwok-Fai So,<sup>2</sup> Zonghua Liu,<sup>1,5</sup> Sufang Zhou,<sup>6</sup> Yongxiang Zhao,<sup>6</sup> Hengwen Yang,<sup>1,5</sup> Libing Zhou,<sup>2,4,7</sup> and Zhinan Yin<sup>1,5</sup>

<sup>1</sup>The First Affiliated Hospital, Biomedical Translational Research Institute and Guangdong Province Key Laboratory of Molecular Immunology and Antibody Engineering, <sup>2</sup>Guangdong-Hong Kong-Macau Institute of CNS Regeneration, Ministry of Education CNS Regeneration Collaborative Joint Laboratory, and

<sup>3</sup>The First Affiliated Hospital, Jinan University, Guangzhou, China

<sup>4</sup>Co-Innovation Center of Neuroregeneration, Nantong University, Jiangsu, China

<sup>5</sup>State Key Laboratory of Biotherapy, Collaborative Innovation Center for Biotherapy, West China Hospital, Sichuan University, Chengdu, China

<sup>6</sup>National Center for International Research of Biological Targeting Diagnosis and Therapy, Guangxi Key Laboratory of Biological Targeting Diagnosis and Therapy Research, Collaborative Innovation Center for Targeting Tumor Diagnosis and Therapy, Guangxi Medical University, Nanning, China

<sup>7</sup>Key Laboratory of Neuroscience, School of Basic Medical Sciences, Institute of Neuroscience, The Second Affiliated Hospital, Guangzhou Medical University, Guangzhou, China

Downloaded from [http://jexpmed.oxfordjournals.org/article/pdf/125/2/521/1758844/jem\\_20170686.pdf](http://jexpmed.oxfordjournals.org/article/pdf/125/2/521/1758844/jem_20170686.pdf) by guest on 08 February 2020

**Immune responses and neuroinflammation are critically involved in spinal cord injury (SCI).  $\gamma\delta$  T cells, a small subset of T cells, regulate the inflammation process in many diseases, yet their function in SCI is still poorly understood. In this paper, we demonstrate that mice deficient in  $\gamma\delta$  T cells ( $TCR\delta^{-/-}$ ) showed improved functional recovery after SCI.  $\gamma\delta$  T cells are detected at the lesion sites within 24 hours after injury and are predominantly of the  $V\gamma4$  subtype and express the inflammatory cytokine IFN- $\gamma$ . Inactivating IFN- $\gamma$  signaling in macrophages results in a significantly reduced production of proinflammatory cytokines in the cerebrospinal fluid (CSF) of mice with SCIs and improves functional recovery. Furthermore, treatment of SCI with anti- $V\gamma4$  antibodies has a beneficial effect, similar to that obtained with anti-TNF- $\alpha$ . In SCI patients,  $\gamma\delta$  T cells are detected in the CSF, and most of them are IFN- $\gamma$  positive. In conclusion, manipulation of  $\gamma\delta$  T cell functions may be a potential approach for future SCI treatment.**

## INTRODUCTION

Spinal cord injury (SCI) is one of the most serious public health problems worldwide and usually results in irreversible sensory, motor, and autonomic impairments (Rubiano et al., 2015). The clinical treatment for SCI is limited to minimizing secondary complications and maximizing residual functions. Experimental strategies have been designed to identify effective approaches that can alleviate secondary damage, reactivate spared circuitry, and rewire the spinal cord after injury (Ramer et al., 2014). Two defined phases are involved in SCI, namely the primary injury and a prolonged secondary injury. The primary injury mechanically damages local cells and the blood–spinal cord barrier (BSCB) and subsequently activates local neuroinflammation and immune responses, which are critically related to the secondary injury (Anwar et al., 2016).

After disruption of the BSCB by a mechanical force that directly destroys neural tissues and endothelial cell membranes, lymphocytes infiltrate the lesion site and drive inflammatory immune responses (Schnell et al., 1999). The inflammation alters the local microenvironment, promotes the release of nitric oxide and reactive oxygen species, and increases BSCB permeability, which further facilitates the entry of peripheral

immune cells and leads to the secondary injury at the lesion site, as well as in the adjacent tissue. Nevertheless, numerous studies have reported neuroprotective and neuroregenerative roles of inflammatory responses that can eliminate tissue debris and induce the release of neurotrophic factors. Recent evidence supports the idea that inflammation has a dual role in SCI: deleterious in the acute injury phase and beneficial in the chronic recovery phase (Ankeny and Popovich, 2009).

IFN- $\gamma$  is a pleiotropic cytokine that exhibits both pro- and antiinflammatory properties (Ottum et al., 2015; Becher et al., 2017). However, the roles of IFN- $\gamma$  in SCI have been somewhat contradictory. It has been reported that IFN- $\gamma$  has a protective effect by reducing the production of chondroitin sulfate proteoglycans and increasing the expression of neurotrophic factors (Fujiyoshi et al., 2010). Additionally, type 1 T helper (Th1) cells are required for the recruitment of tissue-repairing macrophages by secreting IL-10, which is IFN- $\gamma$  dependent (Ishii et al., 2013). Yet, it was noted that IFN- $\gamma$  could activate M1 macrophages, which are harmful to central nervous system (CNS) repairs (Kigerl et al., 2009). As recently reviewed, the dual effect of IFN- $\gamma$  in

\*G. Sun, S. Yang, and G. Cao contributed equally to this paper.

Correspondence to Zhinan Yin: zhinan.yin@yale.edu; Libing Zhou: tlibingzh@jnu.edu.cn

neuroinflammation might depend on the administered dosage, disease phase, and its targets (Becher et al., 2017). Further studies are needed to study the essential source and the effects of IFN- $\gamma$  in SCI.

TNF- $\alpha$  originates mainly from microglia and infiltrated monocytes/macrophages and can also be released by T cells (Kleine et al., 2003; Olmos and Lladó, 2014). Macrophages adopt two functionally antagonistic phenotypes: iNOS $^+$  M1 and CD206 $^+$  M2 (Cusimano et al., 2012; Lech and Anders, 2013). The M1 phenotype is characterized by the excessive release of nitric oxide, IL-1, IL-6, and TNF- $\alpha$ , which leads to toxicity. On the contrary, M2 cells produce immunosuppressive cytokines (e.g., IL-10), stimulate the secretion of growth factors, and thus promote tissue remodeling and repair. Contrary to TNF- $\alpha$ , IFN- $\gamma$  is mainly derived from T cells and facilitates the polarization of M1 macrophages (Gordon and Taylor, 2005; David and Kroner, 2011; Murray et al., 2014).

$\gamma\delta$  T cells have several specific features and unique biological functions (Prinz et al., 2013; Wu et al., 2017) and can be divided into either IFN- $\gamma$  or IL-17 producers (Jensen et al., 2008; Schmolka et al., 2015). We previously reported that  $\gamma\delta$  T cells predominantly produce IFN- $\gamma$ , which is regulated by unique epigenetic and transcription programs (Chen et al., 2007). Peripheral  $\gamma\delta$  T cells are composed of two main subsets: V $\gamma$ 1 and V $\gamma$ 4  $\gamma\delta$  T cells, which have divergent roles in different disease models (Heilig and Tonegawa, 1986; Ito et al., 1989; Pereira et al., 1995). Our group showed that V $\gamma$ 4  $\gamma\delta$  T cells, which produce IFN- $\gamma$ , and V $\gamma$ 1  $\gamma\delta$  T cells, which suppress this function, play divergent roles in tumor immunity (He et al., 2010; Hao et al., 2011). Other groups similarly reported that  $\gamma\delta$  T cells could activate macrophages via IFN- $\gamma$  (Holderness et al., 2013). In addition,  $\gamma\delta$  T cells were considered responsible for recruitment of monocytes/macrophages that boosted innate responses (Bonneville et al., 2010). Additionally, increasing evidence has indicated that  $\gamma\delta$  T cells play critical roles in regulating immune responses in the CNS (Shichita et al., 2009; Benakis et al., 2016; Malik et al., 2016). However, whether  $\gamma\delta$  T cells participate in immune responses after SCI is unknown.

In this paper, we show that  $\gamma\delta$  T cells, especially V $\gamma$ 4  $\gamma\delta$  T cells, play a detrimental role in a mouse model of SCI, probably by providing a critical source of IFN- $\gamma$ , which induces macrophages to adopt the M1 phenotype with increased secretion of proinflammatory cytokines, such as TNF- $\alpha$ . Blocking IFN- $\gamma$  or inactivating V $\gamma$ 4  $\gamma\delta$  T cells with antibodies had a similar effect as that of anti-TNF- $\alpha$  treatment and improved the functional recovery after SCI, which may lead to a new therapeutic approach to SCI.

## RESULTS

### $\gamma\delta$ T cell depletion contributes to functional recovery in a mouse SCI model

Knockout of the *TCR $\delta$*  gene (*TCR $\delta^{-/-}$*  mice) caused a complete loss of  $\gamma\delta$  T cells, with no effect on the development of  $\alpha\beta$  T cells (Itohara et al., 1993), which, using flow cytometry,

was confirmed by showing that few  $\gamma\delta$  T cells were detectable in the mutant spleen (Fig. S1 A). To study the role of  $\gamma\delta$  T cells in functional recovery after SCI, a moderate contusion at the level of the 11th thoracic vertebrae (T11) was made in *TCR $\delta^{-/-}$*  and age-matched WT B6 mice, and the spontaneous recovery of hind limb movement was monitored using the Basso mouse score (BMS; Ung et al., 2007). Both *TCR $\delta^{-/-}$*  and WT animals exhibited complete hind limb paralysis with a BMS score of 0 at 1 d after injury. *TCR $\delta^{-/-}$*  mice recovered gradually: from 5 d after injury, their BMS index increased progressively and peaked at 5 wk after injury (mean of  $5.25 \pm 1.22$ ,  $n = 8$ ; Fig. 1 A). In contrast, functional recovery in WT mice was significantly slower, with a small increase in the BMS index of  $\sim 2.5$  at 2 wk after injury and no further improvements up to 8 wk after injury (Fig. 1 A). This significant difference was also apparent in an increased regularity index (improved walking steps) and enlarged hind max contact area in *TCR $\delta^{-/-}$*  mice 8 wk after injury, compared with control animals ( $75.00 \pm 10.60$  vs.  $47.00 \pm 18.75$  and  $0.161 \pm 0.029$  vs.  $0.089 \pm 0.037$ , respectively,  $n = 8$ ; Fig. 1, B and C). To confirm this, we stimulated the dura mater at the T6 level as reported previously (Baskin and Simpson, 1987) and recorded electromyography of biceps flexor cruris at 8 wk after injury. We found that the amplitudes of motor-evoked potentials (MEPs) were significantly higher in *TCR $\delta^{-/-}$*  than in control mice ( $1.6 \pm 0.86$  vs.  $0.8 \pm 0.44$  mV;  $P < 0.05$ ,  $n = 8$  in each group; Fig. 1 D), indicating a better recovery of electrophysiological functions of injured hind limbs in mutant mice than in control mice. To assess whether structures were preserved better in mutant mice after injury, we first measured the size of spinal cord lesions in serial horizontal sections at 8 wk after injury using anti-glial fibrillary acidic protein (GFAP) immunostaining and found that the lesion volume was significantly smaller in *TCR $\delta^{-/-}$*  than in WT mice ( $0.33 \pm 0.10$  vs.  $0.68 \pm 0.11$  mm $^3$ ;  $P < 0.01$ ,  $n = 6$  animals in each group; Fig. 1 E). We then counted the number of surviving spinal motor neurons using anti-choline acetyltransferase (ChAT) immunostaining at five different levels: the injury site, as well as 1.5 mm and 2.5 mm rostral and caudal. There were no surviving motor neurons at the injury sites in both groups, but more motor neurons survived at the four distant sites in *TCR $\delta^{-/-}$*  mice than in WT mice (Fig. 1 F). As SCI can induce an increase of nonphosphorylated forms of neurofilament H, detected by antibody SMI32 (Pitt et al., 2000), we stained sections with SMI32 and found that the expression in neurons was significantly higher in WT than in *TCR $\delta^{-/-}$*  samples (Fig. 1 G). These results indicated that depletion of  $\gamma\delta$  T cells contributed to motor neuron survival and thereby promoted functional recovery after SCI. To test this hypothesis further,  $\gamma\delta$  T cells from WT mice were isolated and adoptively transferred into *TCR $\delta^{-/-}$*  mice. Using flow cytometry, transferred  $\gamma\delta$  T cells were detectable in mutant spleens 48 h after transplantation (Fig. S1 A). Compared with mice treated with PBS, mice with reconstituted  $\gamma\delta$  T cells exhibited less desirable functional recovery, with significantly

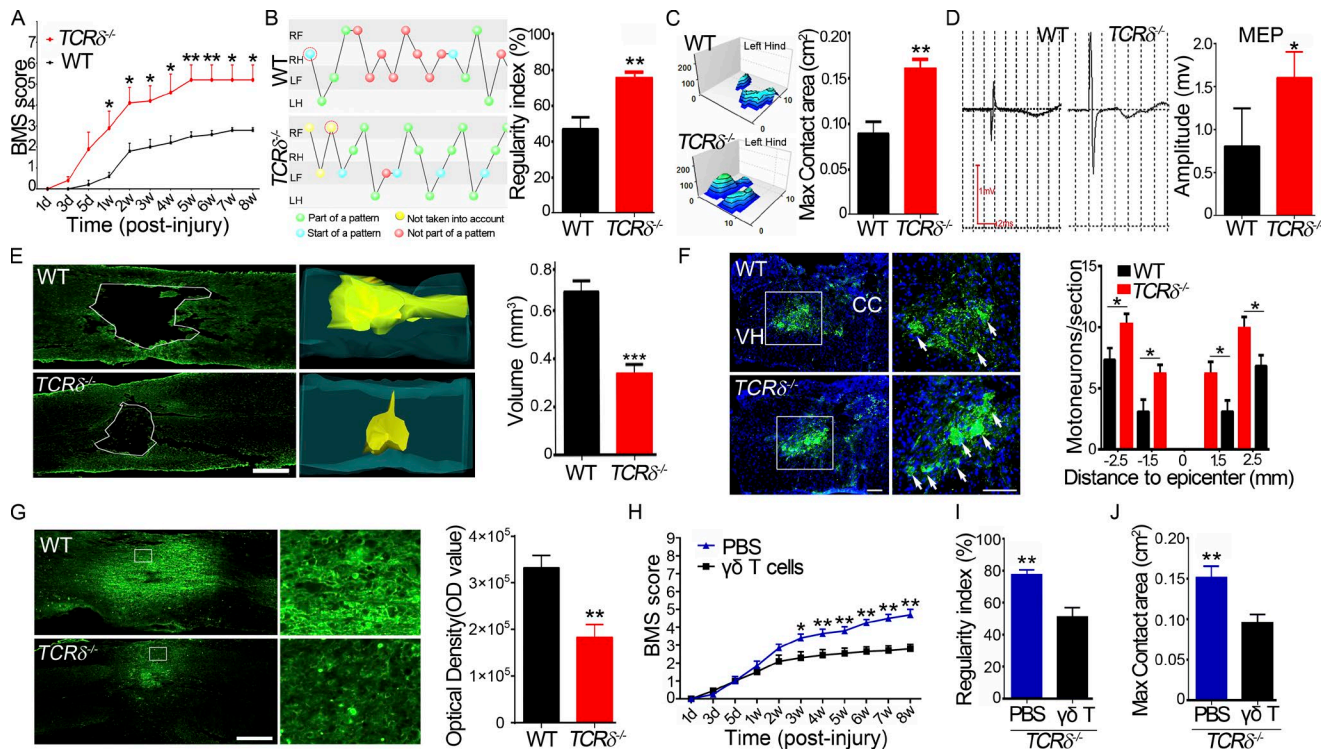


**Figure 1.  $\gamma\delta$  T cells play a detrimental role in traumatic SCI. (A)** BMSs of WT and *TCRδ*<sup>-/-</sup> mice at different time points after spinal cord contusion ( $P < 0.0001$ ,  $n = 8$ ; repeated measures ANOVA with Bonferroni's post-hoc correction). **(B and C)** Locomotor functional recovery evaluated using the CatWalk XT automated quantitative gait analysis system. (B) Regularity index,  $P = 0.0024$ . (C) Hind max contact area,  $P = 0.0065$ . **(D)** Examples and comparison of amplitudes of MEP recordings 8 wk after surgery ( $P = 0.034$ ). (B–D)  $n = 8$ ; Student's *t* test. **(E)** Representative injury sites in WT and *TCRδ*<sup>-/-</sup> animals 8 wk after surgery, labeled with anti-GFAP antibodies, and comparison of lesion volumes in both groups ( $P = 0.0004$ ). Bar, 500  $\mu$ m. **(F)** Survival of motor neurons immunostained with anti-ChAT antibodies in the spinal cord ventral horn at the eighth week after SCI and comparison of ventral horn neurons in both groups at various distances from the injury epicenter ( $P = 0.032$ ). Bars, 250  $\mu$ m. CC, central canal; VH, ventral horn; arrows indicate neurons. (E and F)  $n = 6$ ; Student's *t*-test. **(G)** Anti-SMI32 immunostaining of horizontal spinal sections disclosed more immunoreactivity in the WT than in the mutant 8 wk after surgery ( $P = 0.0028$ ,  $n = 5$ ; Student's *t* test). Bar, 500  $\mu$ m. (F and G) The right panels are magnified from the boxed regions on the left. **(H–J)** Functional recovery of *TCRδ*<sup>-/-</sup> mice after reconstitution with WT  $\gamma\delta$  T cells or injection of PBS ( $n = 6$ ). (H)  $P = 0.0018$  (repeated measures ANOVA with Bonferroni's post-hoc correction). (I)  $P = 0.0002$  (Student's *t* test). (J) Hind max contact area,  $P = 0.0003$  (Student's *t* test). Error bars represent mean  $\pm$  SEM (where included). \*,  $P < 0.05$ ; \*\*,  $P < 0.01$ ; \*\*\*,  $P < 0.001$ .

lower BMSs (Fig. 1 H), regularity index (Fig. 1 I), and hind max contact area (Fig. 1 J) after injury. These results suggested a detrimental role of  $\gamma\delta$  T cells in our mouse model of SCI.

#### $\gamma\delta$ T cells are recruited to the injury site and produce IFN- $\gamma$ in situ

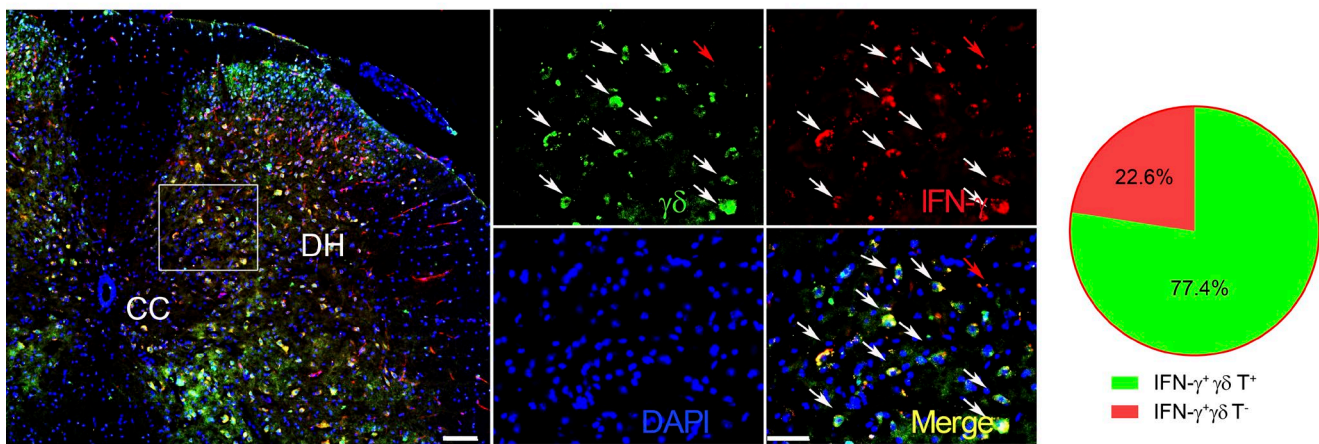
To determine whether  $\gamma\delta$  T cells are recruited into the injury site after SCI, we used *TCRα*<sup>+/−</sup>; *TCRδ*<sup>EGFP/+</sup> mice for an SCI model in which  $\gamma\delta$  T cells were specifically labeled with enhanced GFP (Prinz et al., 2006). As predicted,  $\gamma\delta$  T cells appeared at the injury site 24 h after injury and were quantified. Five slices per mouse and six mice per genotype were quantified. Sections matched in anatomy were serially chosen, and a 0.1-mm<sup>2</sup> area per image was selected randomly (Fu et al., 2017). Most of the IFN- $\gamma$ -positive cells were  $\gamma\delta$  T cells ( $77.4 \pm 2.0\%$ ,  $n = 6$ ; Fig. 2 A). Immunohistochemical staining with anti-V $\gamma$ 1 and -V $\gamma$ 4 antibodies showed that the majority of infiltrating  $\gamma\delta$  T cells ( $91.7 \pm 2.3\%$ ,  $n = 6$ ) were positive for

V $\gamma$ 4, but not for V $\gamma$ 1 (Fig. 2 B). This suggested that V $\gamma$ 4  $\gamma\delta$  T cells might provide an early source of IFN- $\gamma$  in SCI.

#### $\gamma\delta$ T cell-derived IFN- $\gamma$ hampers functional recovery

Based on the results reported (see previous paragraph), we hypothesized that  $\gamma\delta$  T cell-derived IFN- $\gamma$  might be a detrimental mediator in functional recovery after SCI. To test this, *TCRδ*<sup>-/-</sup> mice were reconstituted with *in vivo* expanded  $\gamma\delta$  T cells derived from WT or *IFN-γ*<sup>-/-</sup> mice or injected with PBS 1 d before SCI. The transferred  $\gamma\delta$  T cells were detectable in the spleen of the recipient mice 24 h after transplantation (Fig. S1 A). We found that  $\gamma\delta$  T cells were well reconstituted (Fig. S1 B). *TCRδ*<sup>-/-</sup> mice that received  $\gamma\delta$  T cells from *IFN-γ*<sup>-/-</sup> mice had improved recovery compared with those that received  $\gamma\delta$  T cells from WT mice or those treated with PBS alone, as shown by measuring BMSs (Fig. 3 A), regularity indexes (Fig. 3 B), and greater max contact areas of hind limbs (Fig. 3 C). This was further supported by the observation of

A



B

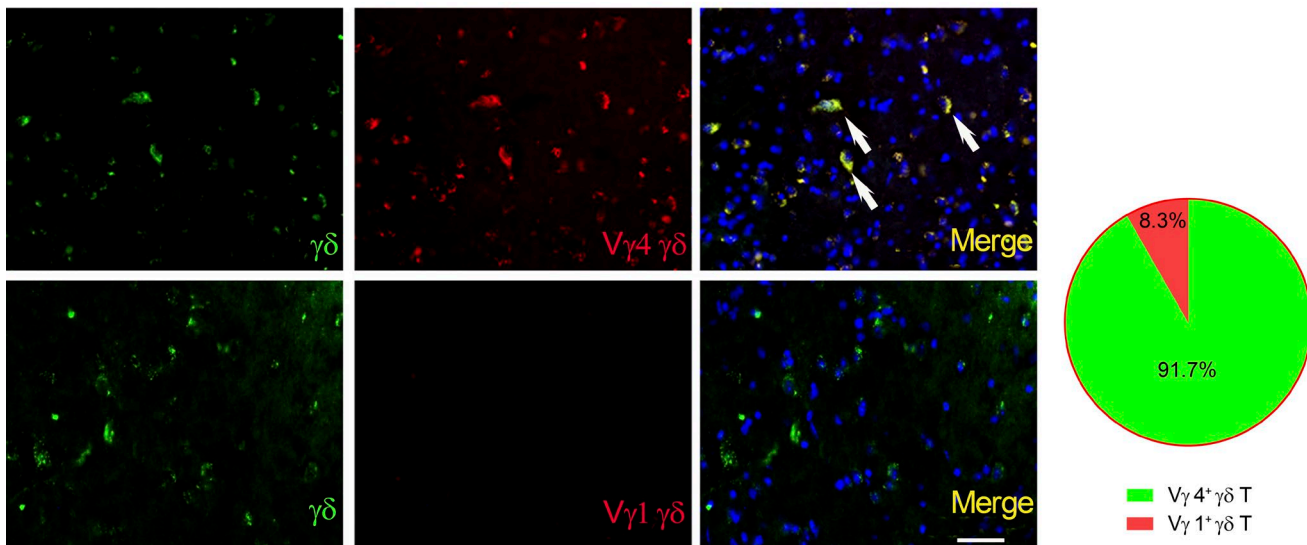


**Figure 2.  $\gamma\delta$  T cells are recruited to the injury site and express IFN- $\gamma$ .** Spinal cord transverse sections from WT mice 24 h after injury. **(A)** TCR  $\delta$ -GFP mice were sacrificed at 24 h after SCI, and spinal cords were prepared for immunohistochemistry. Sections were stained and read by confocal microscopy. DAPI shows the nucleus. The percentage of  $\gamma\delta$  T cells and non- $\gamma\delta$  T cells in total IFN- $\gamma$ <sup>+</sup> cells was calculated and is shown in the pie chart. White arrows point to IFN- $\gamma$ -producing  $\gamma\delta$  T cells. Red arrows point to IFN- $\gamma$ <sup>+</sup>  $\gamma\delta$  T cells. CC, central canal; DH, dorsal horn. **(B)** Double immunofluorescence showed that most  $\gamma\delta$  T cells were V $\gamma$ 4 positive (indicated by arrows), but not V $\gamma$ 1 positive. Bars, 50  $\mu$ m.  $n = 6$  mice per group. One representative of at least two independent experiments is shown.

smaller lesions and an increased number of surviving motor neurons in the group reconstituted with IFN- $\gamma$ <sup>-/-</sup>  $\gamma\delta$  T cells versus the group with WT  $\gamma\delta$  T cells (Fig. S2). These results indicated that IFN- $\gamma$  might be a critical mediator involved in the detrimental effects of  $\gamma\delta$  T cells in SCI.

To define which subset of  $\gamma\delta$  T cells was the main source of IFN- $\gamma$ , V $\gamma$ 4  $\gamma\delta$  T cells or V $\gamma$ 1  $\gamma\delta$  T cells from WT or IFN- $\gamma$ <sup>-/-</sup> mice or PBS as a control were transferred into TCR $\delta$ <sup>-/-</sup> mice 1 d before SCI. TCR $\delta$ <sup>-/-</sup> mice reconstituted with V $\gamma$ 4  $\gamma\delta$  T cells from IFN- $\gamma$ <sup>-/-</sup> mice or injected with PBS displayed better functional recovery than those reconstituted with WT V $\gamma$ 4  $\gamma\delta$  T cells, as shown in BMSs

and CatWalk tests (Fig. 3, D–F). Interestingly, this effect was not obtained with V $\gamma$ 1  $\gamma\delta$  T cells: TCR $\delta$ <sup>-/-</sup> mice reconstituted with WT V $\gamma$ 1  $\gamma\delta$  T cells, IFN- $\gamma$ <sup>-/-</sup> V $\gamma$ 1  $\gamma\delta$  T cells, or PBS had similar functional recoveries (Fig. 3, G–I). These results strongly suggest that V $\gamma$ 4  $\gamma\delta$  T cells are the earliest source of IFN- $\gamma$  after SCI.

#### IFN- $\gamma$ signaling is critical for the functional impairment after SCI

To further evaluate whether IFN- $\gamma$  acts as a key mediator in  $\gamma\delta$  T cell–induced impairment of recovery, experimental SCI was performed in IFN- $\gamma$ <sup>-/-</sup> and IFN- $\gamma$ R<sup>-/-</sup> mice. As

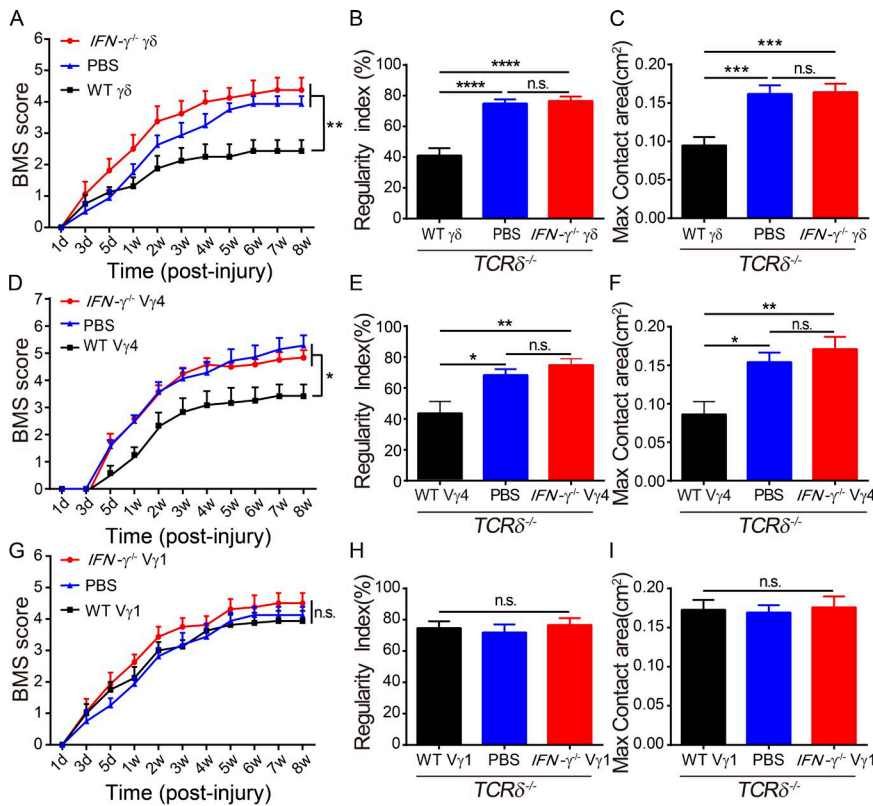


Figure 3.  $\gamma\delta$  T cell-derived IFN- $\gamma$  is critical in impairing recovery after SCI. (A–C)  $TCR\delta^{-/-}$  SCI mice were reconstituted with  $\gamma\delta$  T cells from WT or  $IFN-\gamma^{-/-}$  animals or PBS alone, and evaluation of recovery after SCI. (D–F) Functional recovery of  $TCR\delta^{-/-}$  SCI mice reconstituted with  $V\gamma 4$   $\gamma\delta$  T cells from WT or  $IFN-\gamma^{-/-}$  mice or PBS only. (G–I) Recovery after SCI of  $TCR\delta^{-/-}$  SCI mice reconstituted with  $V\gamma 1$   $\gamma\delta$  T cells from WT or  $IFN-\gamma^{-/-}$  mice or PBS only. Error bars represent mean  $\pm$  SEM. (A, D, and G) Two-way repeated measures ANOVA with Bonferroni's post-hoc correction. (B, C, E, F, H, and I) One-way ANOVA with Tukey's multiple comparisons test. \*  $P < 0.05$ ; \*\*  $P < 0.01$ ; \*\*\*  $P < 0.001$ ; \*\*\*\*  $P < 0.0001$ . n.s., not significant.  $n = 8$ .

expected,  $IFN-\gamma^{-/-}$  and  $IFN-\gamma R^{-/-}$  mice recovered better than control mice, as indicated by higher BMSs, increased regularity indexes, and larger max contact areas of hind limbs (Fig. 4, A–C). These results were consistent with the previous

findings that IFN- $\gamma$ -stimulated M1 macrophages were detrimental to neurons in vitro (Kigerl et al., 2009).

To determine whether macrophages were critical IFN- $\gamma$  responders in vivo, a bone marrow chimera assay and adoptive

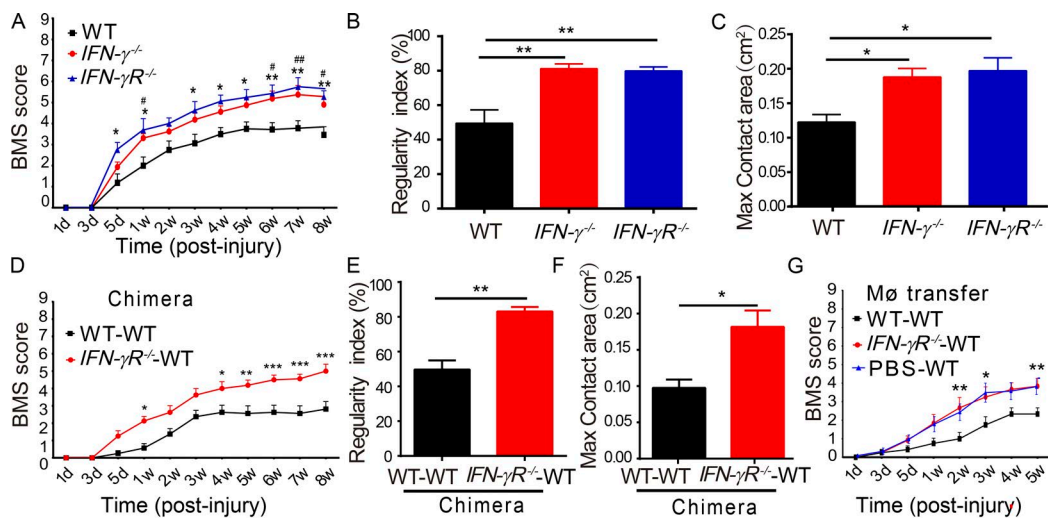


Figure 4. IFN- $\gamma$  signaling in macrophages is essential for impairing neurological recovery from SCI. (A–C) After SCI, behavioral tests were assessed in WT,  $IFN-\gamma^{-/-}$ , and  $IFN-\gamma R^{-/-}$  mice. (A) Statistical analysis comparing  $IFN-\gamma^{-/-}$  and WT mice (\*, \*\*) or  $IFN-\gamma R^{-/-}$  and WT (#, ##). (B and C) Regularity index and hind max contact area with CatWalk test. (D–F) Irradiated WT mice were reconstituted with bone marrow from WT or  $IFN-\gamma R^{-/-}$  mice and tested for recovery. (G) BMSs were measured in irradiated WT mice injected with peritoneal macrophages prepared from WT or  $IFN-\gamma R^{-/-}$  mice or PBS alone. Error bars represent mean  $\pm$  SEM. (A, D, and G) Two-way repeated measures ANOVA with Bonferroni's post-hoc correction. (B, C, E, and F) One-way ANOVA with Tukey's multiple comparisons test. \* or #,  $P < 0.05$ ; \*\* or ##,  $P < 0.01$ ; \*\*\*,  $P < 0.001$ .  $n = 8$ .  $M_0$ , macrophages.

transfer experiments were performed. For the chimera assay, bone marrow cells from WT or *IFN-γR*<sup>-/-</sup> mice were transplanted into irradiated WT mice, and chimeric mice were found to have ~85% chimeric cells (Fig. S1 D), indicating a successful reconstitution. The chimeric mice that received *IFN-γR*<sup>-/-</sup> bone marrow cells exhibited better functional recovery than those that received WT bone marrow cells, as shown in BMSs and CatWalk tests (Fig. 4, D–F). This indicated that bone marrow–derived cells were the IFN-γ responders after SCI. For adoptive transfer experiments, peritoneal macrophages were collected from WT or *IFN-γR*<sup>-/-</sup> mice and transferred into WT mice by intravenous injections (Wang et al., 2015). Compared with mice that received WT macrophages, those that received *IFN-γR*<sup>-/-</sup> macrophages recovered better in terms of BMSs (Fig. 4 G) and CatWalk tests (Fig. S3). Thus, bone marrow–derived macrophages (BMDMs) are likely the main responders to IFN-γ signaling and impair recovery after SCI.

#### γδ T cell–derived IFN-γ regulates the production of proinflammatory cytokines

We then asked whether the depletion of γδ T cells or inactivation of IFN-γ functions influences the production of proinflammatory cytokines. Spinal cord tissues from the injury sites were collected 24 h after injury, and the levels of different cytokines were measured using a multiplex Luminex kit. In samples from *TCRδ*<sup>-/-</sup> mice, the levels of M1-related proinflammatory cytokines, including IL-1α, IL-6, TNF-α, IFN-γ, and MIP-1α, were significantly decreased when compared with samples from WT mice or from *TCRδ*<sup>-/-</sup> mice reconstituted with WT γδ T cells (Fig. 5 A and Fig. S4). These proinflammatory cytokines were also significantly reduced in lesioned spinal cord tissue from *IFN-γ*<sup>-/-</sup> and *IFN-γR*<sup>-/-</sup> mice (Fig. 5 B and Fig. S4). To test whether inactivation of IFN-γ signaling affects macrophage phenotypes, 24 h after SCI, tissue sections were immunostained with anti-F4/80, a generic macrophage marker, and with anti–nitric oxide synthase (iNOS), a marker of the M1 phenotype. The ratio of iNOS- to F4/80-positive cells was used to estimate the proportion of M1-activated macrophages. As shown in Fig. 5 C, most infiltrating macrophages in WT mice were iNOS positive, showing an M1 phenotype (Prieur et al., 2011). In contrast, the proportion of iNOS-positive cells was reduced in *IFN-γR*<sup>-/-</sup> mice (Fig. 5 C). Additionally, some Arg1-positive cells, presumably M2 macrophages, were present in spinal sections from *IFN-γR*<sup>-/-</sup> mice (Fig. S5). These results further supported the fact that γδ T cells produced early IFN-γ-stimulated proinflammatory M1 macrophages and induced detrimental effects in SCI.

Transcription factor NF-κB is critical in regulating the expression of numerous proinflammatory cytokines such as TNF-α and IL-6, and its phosphorylation induces the production of these detrimental cytokines after SCI (Mattson and Camandola, 2001). To test whether the changes of cytokine levels observed upon IFN-γ inactivation were re-

lated to NF-κB signaling, we isolated macrophages from WT and *IFN-γR*<sup>-/-</sup> mice and stimulated them with lipopolysaccharide. Western blot analysis showed that the phosphorylation of NF-κB p65 (Ser 468) and Stat1 was significantly less in *IFN-γR*<sup>-/-</sup> mice when compared with WT control mice (Fig. 5 D).

#### Anti-Vγ4 treatment improves functional recovery after SCI

Having determined that Vγ4 γδ T cells are the main source of IFN-γ at the SCI injury site and that IFN-γ favors the production of proinflammatory cytokines that hinder recovery, we hypothesized that Vγ4 γδ T cells might serve as a potential target for therapy after SCI. To test this, WT mice with SCI were treated with anti-Vγ4 antibodies, and their neurological functional recoveries were monitored as described in the previous paragraph. Using flow cytometry analysis of spleen samples, we detected 21.5% Vγ4-positive cells and 49.5% Vγ1-positive cells among all γδ T cells from control antibody–treated mice; however, the percentages were reduced to 1.19% in anti-Vγ4 antibody–treated mice and 7.26% in anti-Vγ1–treated mice, respectively (Fig. S1 C), indicating that antibodies effectively inactivated Vγ4- or Vγ1-positive cells. Anti–TNF-α treatment, previously known to be beneficial in SCI, was used as a positive control. Treatment with anti-Vγ4, anti–IFN-γ, or anti–TNF-α antibodies had similar effects and resulted in significantly better recoveries when compared with treatment with control antibody or anti-Vγ1 antibodies, which yielded comparable results, as estimated in the BMS and CatWalk tests (Fig. 6, A–C).

#### Traumatic SCI in human subjects induces the infiltration of γδ T cells

To investigate whether lesion infiltration with γδ T cells also occurs in patients with SCI, cerebrospinal fluid (CSF) samples were collected from 22 patients with thoracic or cervical segment injuries (Fig. 7 B and Table 1) and from 20 control donors without SCI. Using flow cytometry analysis, γδ T cells were detected in the CSF or the peripheral blood from patients ( $n = 15$ ; Fig. 7 A), but not in controls ( $n = 3$ ; Fig. S1 D). Interestingly, we found detectable levels of IFN-γ, but not IL-17, in the CSF and blood from SCI patients (Fig. 7 A and Fig. S1 D). Furthermore, the level of IFN-γ from CSF-derived γδ T cells was significantly higher than that from blood-derived γδ T cells (Fig. 7, B and C;  $n = 15$  patients). Levels of proinflammatory cytokines IFN-γ, IL-6, TNF-α, MIP-1β, and MCP-1 were significantly increased in the CSF of SCI patients ( $n = 22$ ) compared with controls ( $n = 20$ ; Fig. 7 D). Our results from human samples thus confirm the conclusion from our animal studies that γδ T cells were the source of IFN-γ in SCI.

#### DISCUSSION

Neurological impairment after SCI is a severe health problem that is aggravated by the infiltration of immune cells and the resulting inflammation at and around the injury site. Our

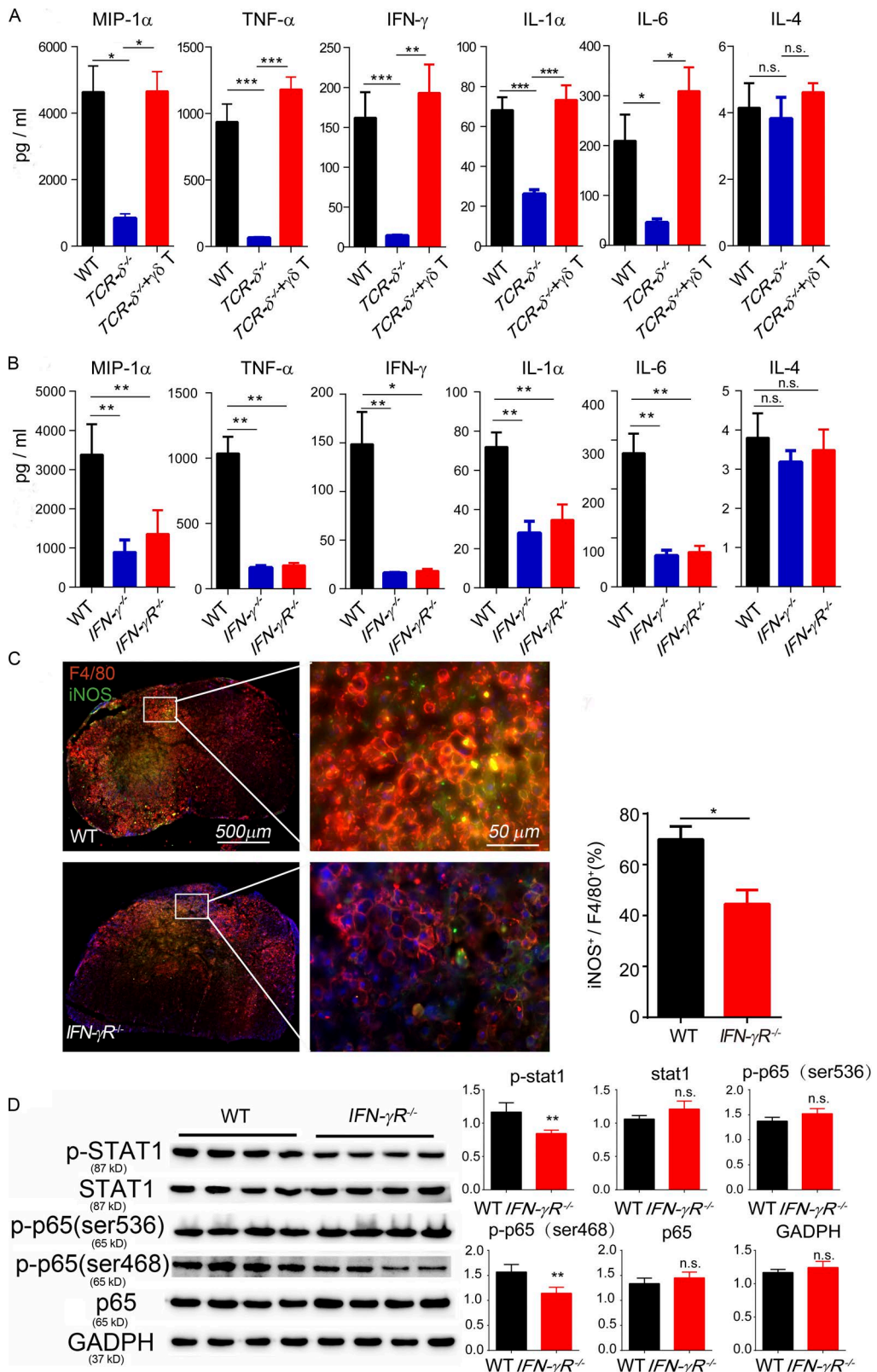


**Figure 5.  $\gamma\delta$  T cells and IFN- $\gamma$  influence the production of proinflammatory cytokines at the SCI site.** Proinflammatory cytokines were analyzed in spinal samples at 1 d after SCI. **(A)** The levels of MIP-1 $\alpha$ , TNF- $\alpha$ , IFN- $\gamma$ , IL-1 $\alpha$ , and IL-6 were significantly decreased in the  $TCR\delta^{-/-}$  group compared with the WT or  $TCR\delta^{-/-}$  plus  $\gamma\delta$  T cell reconstitution groups. IL-4 expression was comparable in the three groups (one-way ANOVA with Tukey's multiple comparisons

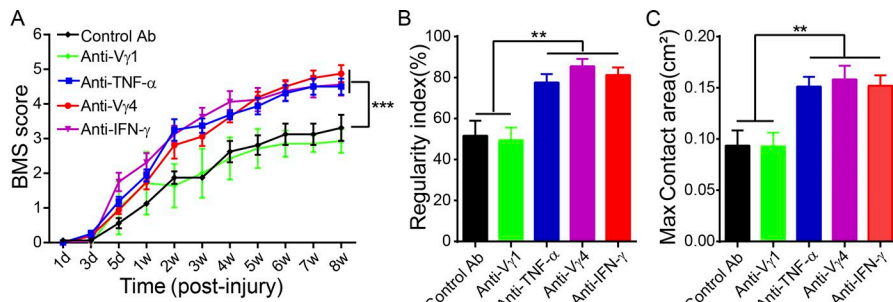


**Figure 6. Anti-V $\gamma$ 4 or anti-IFN- $\gamma$  treatment contributes to functional recovery after SCI.** WT SCI animals were treated with anti-IFN- $\gamma$ , anti-TNF- $\alpha$ , anti-V $\gamma$ 4, and anti-V $\gamma$ 1 antibodies or isotype antibodies as control and underwent behavioral tests. **(A–C)** BMSs (A) were estimated at different time points after injury ( $P < 0.0001$ ; two-way repeated measures ANOVA with Bonferroni's post-hoc correction), and regularity index (B) and max contact area (C; one-way ANOVA with Tukey's multiple comparisons test) were measured with CatWalk at the eighth week after injury.  $n = 8$  mice per group; mean  $\pm$  SEM; \*\*,  $P < 0.01$ ; \*\*\*,  $P < 0.001$ , all compared with the control antibody group.

research shows that  $\gamma\delta$  T cells, especially V $\gamma$ 4  $\gamma\delta$  T cells, are recruited at the injury site during the early phase after SCI, which impairs functional recovery. IFN- $\gamma$  secreted by V $\gamma$ 4  $\gamma\delta$  T cells acts on BMDMs, triggering their production of TNF- $\alpha$  and other cytokines. Inactivation of V $\gamma$ 4  $\gamma\delta$  T cells or blocking of IFN- $\gamma$  functions results in functional improvement comparable to that obtained with anti-TNF- $\alpha$  treatment, further confirming a detrimental role of V $\gamma$ 4  $\gamma\delta$  T cells in SCI. Detection of IFN- $\gamma$ -producing  $\gamma\delta$  T cells in the CSF and peripheral blood of SCI patients lends further support to our hypothesis. Therefore, our studies demonstrate a previously unknown, physiopathological mechanism of neurological impairment after SCI and identify V $\gamma$ 4  $\gamma\delta$  T cells as novel potential therapeutic targets.

$\gamma\delta$  T cells are a unique subset of T cells that play different roles in different disease models. For example,  $\gamma\delta$  T cells prevented the overproduction of inflammatory cytokines in the *Listeria monocytogenes*-infected mouse model (Skeen et al., 2001), whereas they provided a major source of inflammatory cytokines detrimental to the injury in an ischemic model (Shichita et al., 2009). They also harbored different roles in different tumor models (Gao et al., 2003; Daley et al., 2016). A striking observation in our study was that complete depletion of  $\gamma\delta$  T cells resulted in improved neurological recovery from experimental SCI in mice and that recovery in *TCR $\delta$ <sup>-/-</sup>* mice was very similar to that in *IFN- $\gamma$ <sup>-/-</sup>* mice (Fig. 1 and Fig. 3), indicating that  $\gamma\delta$  T cells may provide the main source of IFN- $\gamma$  in SCI. Indeed,  $\gamma\delta$  T cells, especially IFN- $\gamma$ -positive V $\gamma$ 4  $\gamma\delta$  T cells, are recruited at the injury site (Fig. 2), and the reconstitution of *TCR $\delta$ <sup>-/-</sup>* mice with V $\gamma$ 4  $\gamma\delta$  T cells isolated from *IFN- $\gamma$ <sup>-/-</sup>* mice, but

not from WT mice (Fig. 3), enhanced neurological recoveries. This is in agreement with the idea that V $\gamma$ 4  $\gamma\delta$  T cells provide an early source of IFN- $\gamma$  in SCI and play a detrimental role in neurological recoveries. However, we cannot exclude the possibility that  $\gamma\delta$  T cells might also contribute to the immunopathology upon injury. It also remains unclear which factors trigger the recruitment of V $\gamma$ 4  $\gamma\delta$  T cells at the injury sites, whether the IFN- $\gamma$ -producing  $\gamma\delta$  T cells are selectively recruited, and how they are triggered to produce IFN- $\gamma$ . SCI broke the BSCB, and this may have caused the release of different cytokines and chemokines. Further studies are needed to better identify the factors responsible for the recruitment and activation of  $\gamma\delta$  T cells in SCI.

The effect of IFN- $\gamma$  on CNS inflammation and repair is still controversial. Using genetic animal models, we provide convincing evidence that the early production of IFN- $\gamma$  by  $\gamma\delta$  T cells is detrimental for recovery after SCI and that BMDMs are key responders to IFN- $\gamma$ . In addition, we found an early filtration of  $\gamma\delta$  T cells with the elevated level of IFN- $\gamma$  in the CSF from SCI patients, further supporting our hypothesis that IFN- $\gamma$  influences the outcome of neuronal injury. Furthermore, other studies using *IFN- $\gamma$ <sup>-/-</sup>* mice also demonstrated a neurotoxic effect of IFN- $\gamma$  after peripheral nerve injuries (Victório et al., 2012). A detrimental role of IFN- $\gamma$  produced by Th1 cells has also been suggested in other CNS diseases (Smith et al., 2009; Silver et al., 2015). We are aware that our data appear contradictory to observations that administration of IFN- $\gamma$  has a protective role after SCI (Fujiyoshi et al., 2010; Ishii et al., 2013). This apparent discrepancy might be caused by the different techniques used to produce and analyze SCI in mice. In this, it is worth noting that the putative

test). **(B)** In the *IFN- $\gamma$ <sup>-/-</sup>* and *IFN- $\gamma$ R<sup>-/-</sup>* group, the levels of MIP-1 $\alpha$ , TNF- $\alpha$ , IFN- $\gamma$ , IL-1 $\alpha$ , and IL-6 were significantly decreased compared with the WT group, but there were no significant differences between the *IFN- $\gamma$ <sup>-/-</sup>* and *IFN- $\gamma$ R<sup>-/-</sup>* groups (one-way ANOVA with Tukey's multiple comparisons test). **(C)** Spinal sections from WT mice 1 wk after SCI immunostained with anti-F4/80 (a generic marker for macrophages) and anti-iNOS (a marker for M1 macrophages). The ratio of iNOS-positive to F4/80-positive cells was significantly decreased in the *IFN- $\gamma$ R<sup>-/-</sup>* group compared with the WT ( $P = 0.0113$ ). **(D)** Protein expression was analyzed by Western blot using BMDMs from WT and *IFN- $\gamma$ R<sup>-/-</sup>* mice followed with lipopolysaccharide stimulation. The phosphorylation of Stat1 and p65 was significantly decreased in the *IFN- $\gamma$ R<sup>-/-</sup>* group compared with the WT (Student's *t* test). \*,  $P < 0.05$ ; \*\*,  $P < 0.01$ ; \*\*\*,  $P < 0.001$ . Results (C) represent one of at least two repeated experiments; mean  $\pm$  SEM;  $n = 4$ . n.s., not significant.

protective role of IFN- $\gamma$  in these experiments was not tested directly in *IFN- $\gamma$ <sup>-/-</sup>* or *IFN- $\gamma$ R<sup>-/-</sup>* mice. The differences in the approaches and time points of interfering IFN- $\gamma$  signaling might also have contributed to the discrepancies.

Macrophages are key regulators of balanced pro- and antiinflammatory responses. According to the microenvironment, macrophages can adopt two phenotypes: classically (M1) or alternatively (M2) activated macrophages (Murray et al., 2014). Macrophages adopt the M1 phenotype upon stimulation with IFN- $\gamma$ , plus bacterial products such as lipo-polysaccharide. IFN- $\gamma$  induces secretion by M1 macrophages of inflammatory cytokines including TNF- $\alpha$ , IL-1, and IL-6 (David and Kroner, 2011). M2 macrophages, induced by Th2 cytokines such as IL-4 and IL-13, as well as by immune complexes, produce antiinflammatory cytokines, inhibit the inflammation response, and promote tissue repair (Gordon and Taylor, 2005). One important finding of our studies was that BMDMs are the responders to V $\gamma$ 4-derived IFN- $\gamma$  and are a main source of proinflammatory cytokines. This is supported by two sets of observations. First, *IFN- $\gamma$ R<sup>-/-</sup>* mice, chimeras with *IFN- $\gamma$ R<sup>-/-</sup>* bone marrow, as well as mice receiving adoptively transferred *IFN- $\gamma$ R<sup>-/-</sup>* peritoneal macrophages show similar functional recoveries after SCI (Fig. 4). However, we cannot exclude the possibility that the adoptively transferred macrophages might possess different abilities to traffic to the lesion sites. Second, levels of proinflammatory cytokines and numbers of M1 macrophages are reduced in *IFN- $\gamma$ <sup>-/-</sup>* mice compared with WT mice (Fig. 5 A). We present consistent results that inflammatory cytokines in *TCR $\delta$ <sup>-/-</sup>*, *IFN- $\gamma$ <sup>-/-</sup>*, and *IFN- $\gamma$ R<sup>-/-</sup>* mice are more significantly reduced than WT mice in the SCI model (Fig. 5, A and B), further supporting our notion that  $\gamma\delta$ T cells provide the earliest source of IFN- $\gamma$  that triggers the production of inflammatory cytokines by macrophages in an IFN- $\gamma$ -IFN- $\gamma$ R-dependent manner. By regulating the production of proinflammatory cytokines, the NF- $\kappa$ B pathway plays a central role in controlling inflammation (Libermann and Baltimore, 1990; Beg et al., 1993; Beg and Baltimore, 1996; Sumitomo et al., 1999; Luan et al., 2014; Yu et al., 2015), and we show reduced NF- $\kappa$ B p65 phosphorylation in *IFN- $\gamma$ R<sup>-/-</sup>* macrophages (Fig. 5 D). In the presence of IFN- $\gamma$ , cytokines released from damaged spinal cords may trigger NF- $\kappa$ B activation and production of proinflammatory cytokines. This could result in a positive loop, accounting for the “secondary hit” of SCI. In contrast, a decrease in IFN- $\gamma$  signaling may down-regulate the NF- $\kappa$ B pathway, interrupting that positive loop and thus showing improved neurological recovery.

Based on the fact that V $\gamma$ 4  $\gamma\delta$ T cells are the key source of IFN- $\gamma$ , which then triggers detrimental inflammatory cytokine production by macrophages and increases neurological injury, it is certainly possible that V $\gamma$ 4  $\gamma\delta$ T cells are the potential target for in vivo intervention. Indeed, we used a V $\gamma$ 4  $\gamma\delta$  TCR-specific antibody (clone UC3) in vivo and showed that injection of neutralizing anti-V $\gamma$ 4 antibodies has a beneficial effect of neurological recovery upon SCI (Fig. 6). Although

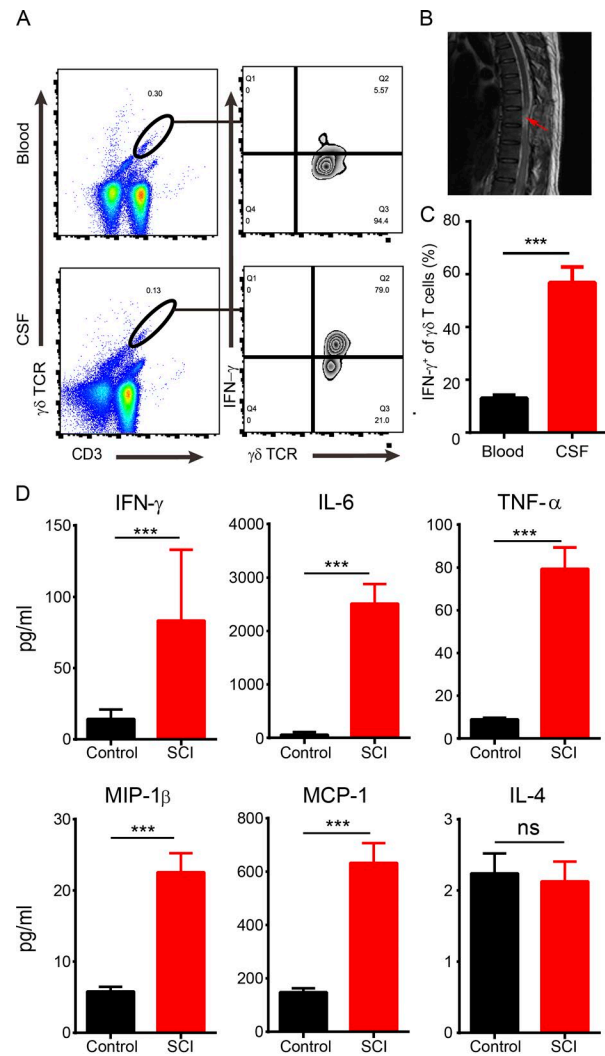


**Figure 7. Infiltration of  $\gamma\delta$  T cells and elevated levels of inflammatory cytokines in the CSF of SCI patients.** **(A)** Using flow cytometry analysis,  $\gamma\delta$  T cells were enriched in the CSF and peripheral blood from SCI patients, and most of CSF-derived  $\gamma\delta$  T cells were positive for IFN- $\gamma$ . **(B)** MRI image showing the injury site in a patient with SCI (arrow). **(C)** Statistical analysis showed a significantly higher ratio of IFN- $\gamma$ <sup>+</sup>  $\gamma\delta$  T cells in CSF than peripheral blood samples ( $P < 0.0001$ ;  $n = 15$ ). **(D)** The levels of IFN- $\gamma$ , IL-6, TNF- $\alpha$ , MIP-1 $\beta$ , and MCP-1, but not IL-4, were significantly increased in the CSF from SCI patients compared with the control group ( $n = 20-22$ ). Numbers represent frequencies (percentage) of cells in corresponding gates. Results (A and B) represent one of at least two repeated experiments. \*\*\* $P < 0.01$ . Mean  $\pm$  SEM; Student's *t* test; ns, not significant.

there is evidence showing that anti-pan  $\gamma\delta$  TCR antibody (clone UC7) induces TCR internalization rather than depleting the cells (Koenecke et al., 2009), it remains unclear whether anti-V $\gamma$ 1 (clone 2.11) or anti-V $\gamma$ 4 antibodies deplete the corresponding subset of  $\gamma\delta$  T cells or just inactivate them. However, these two antibodies have been widely used in vivo to inactivate these two subsets of  $\gamma\delta$  T cells in many disease models (Huber et al., 2000; Hahn et al., 2004; Huang

Table 1. Patient demographics and baseline neurological status

ID	Mechanism of injury	Spinal injury	Age	Sex	ASIA grade	Level
1	MVA	T9/T10 fracture-dislocation	45	M	A	Thoracic
2	Fall from standing height	T4 burst fracture	21	M	A	Thoracic
3	Diving	C6/7 fracture-dislocation	36	M	B	Cervical
4	MVA	C4/5 fracture-dislocation	28	F	A	Cervical
5	Fall from standing height	C5/6 flexion-distraction	39	M	B	Cervical
6	Fall from standing height	T9 and T10 burst fractures	41	F	B	Thoracic
7	MVA	T10 burst fracture	32	M	A	Thoracic
8	MVA	T1 burst fracture	25	M	A	Thoracic
9	MVA	T6 burst fracture	33	M	A	Thoracic
10	MVA	T12 burst fracture	50	M	A	Thoracic
11	Fall from standing height	T8 burst fracture	46	M	B	Thoracic
12	MVA	C6/7 fracture-dislocation	33	M	A	Cervical
13	MVA	T11/T11 fracture-dislocation	26	F	A	Thoracic
14	MVA	T6 and T7 burst fractures	36	M	A	Thoracic
15	MVA	T8 and T9 burst fractures	42	M	A	Thoracic
16	Fall from standing height	T8 and T9 burst fractures	31	M	A	Thoracic
17	Fall from standing height	C5/6 flexion-distraction	30	F	B	Cervical
18	Fall from standing height	C3/4 flexion-distraction	37	M	A	Cervical
19	MVA	C5/6 flexion-distraction	36	M	A	Cervical
20	MVA	T1 burst fracture	35	M	B	Thoracic
21	MVA	T10 burst fracture	22	F	A	Thoracic
22	MVA	T7 burst fracture	28	M	A	Thoracic
Totals			34.18 ± 7.69	17 M, 5 F	16 A, 6 B	7 cervical, 15 thoracic

MVA, motor vehicle accident; M, male; F, female.

et al., 2009; Hao et al., 2011). Our results further emphasize that antibodies against V $\gamma$ 4  $\gamma\delta$  T cells inactivate the function of this subset of  $\gamma\delta$  T cells.

The inflammatory cytokine TNF- $\alpha$  is considered a therapeutic target in autoimmune diseases, and anti-TNF- $\alpha$  antibodies have been used successfully in Crohn's disease, ulcerative colitis, psoriasis, psoriatic arthritis, ankylosing spondylitis, and rheumatoid arthritis (Prescott et al., 2007; Kemény-Beke et al., 2010; Papoutsaki and Costanzo, 2013; Mozaffari et al., 2014; Ceccarelli et al., 2017; Rayen et al., 2017). It was also shown that treatment with anti-TNF- $\alpha$  is beneficial in animal SCI models (Genovese et al., 2006, 2007; Marchand et al., 2009; Bayrakli et al., 2012). In our model, the improved recovery observed in the absence of  $\gamma\delta$  T cells, especially V $\gamma$ 4  $\gamma\delta$  T cells and their production of IFN- $\gamma$ , is very similar to the effect of anti-TNF- $\alpha$  treatment (Fig. 6), and this suggests that V $\gamma$ 4  $\gamma\delta$  T cells are a potential therapeutic target in SCI. This is further supported by our demonstration that human samples from SCI patients are enriched in IFN- $\gamma$ -positive  $\gamma\delta$  T cells and inflammatory cytokines (Fig. 7). Further studies are needed to understand future links between  $\gamma\delta$  T cell-derived IFN- $\gamma$ , the consequential production of inflammatory cytokines, and the mechanisms of functional recovery.

In summary, as revealed in our mouse model,  $\gamma\delta$  T cells, especially V $\gamma$ 4  $\gamma\delta$  T cells, play a detrimental role in the acute phase of SCI by providing IFN- $\gamma$  that acts on BMDMs and directs them toward M1 phenotypes; these phenotypes in turn produced proinflammatory cytokines. Treatment with

neutralizing V $\gamma$ 4 antibodies shows a beneficial effect similar to that of anti-TNF- $\alpha$ . Therefore, V $\gamma$ 4  $\gamma\delta$  T cells should be considered as a novel therapeutic target for SCI.

## MATERIALS AND METHODS

### Mice

C57BL/6J,  $TCR\delta^{-/-}$ ,  $IFN-\gamma^{-/-}$ ,  $IFN-\gamma R^{-/-}$ , and  $TCR\alpha^{+/-}$ ;  $TCR\delta^{EGFP/+}$  mice were purchased from the Jackson Laboratory. All mice were females, aged 7–8 wk old, and weighed 17–22 g at the time of surgery. Animals were maintained under pathogen-free conditions in the animal facility at Jinan University. All procedures were approved by and performed in accordance with the Jinan University's Institutional Laboratory Animal Care and Use Committee.

### Reagents

PerCP-conjugated anti-mouse CD11c (clone N418) was purchased from BioLegend. PE-conjugated anti-mouse F4/80 (clone BM8), APC-conjugated anti-mouse CD86 (clone GL1), and FITC anti-mouse TNF- $\alpha$  (clone XT3.11) were purchased from Tianjin Sungene. GolgiPlugs were purchased from BD Biosciences. Anti-mouse CD3e mAb (clone 145-2C11), anti-mouse CD28 mAb (clone 37.51), and purified hamster IgG anti-mouse TCR V $\gamma$ 1 (clone 2.11)/V $\gamma$ 4 (clone UC3)/TCR- $\gamma$ / $\delta$  (clone GL3) mAb were from Tianjin Sungene. The recombinant human TNF- $\alpha$  receptor IgG Fc fusion protein (rhTNFR:Fc) was obtained from Shanghai CP Guojian Pharmaceutical Co., Ltd. Antibodies used for  $\gamma\delta$  T cell flow cytometric analysis such as FITC

anti-mouse TCR V $\gamma$ 1 (clone 2.11), PE anti-mouse TCR V $\gamma$ 4 (clone UC3-10A6), APC anti-mouse TCR- $\gamma$ / $\delta$  (clone GL3), PerCP/Cy5.5 anti-human TCR- $\gamma$ / $\delta$  (clone GL3), and FITC anti-human IFN- $\gamma$  (clone B27) were purchased from Tianjin Sungene. PerCP/Cy5.5 anti-human TCR- $\gamma$ / $\delta$  (clone B1), V500 anti-human CD3 (clone SP34-2), and V450 anti-mouse CD3 (clone 500A2) were from BD Biosciences, and PE anti-human IL-17A (clone BL168) was from BioLegend. The standard culture medium was RPMI 1640 (Euroclone) or DMEM (Hyclone; Thermo) containing 10% FCS (Euroclone), 2 mM L-glutamine, 100 U/ml penicillin, and 100 mg/ml streptomycin.

### Contusive SCI model

Contusive SCI was performed using a New York University impactor as described previously (Ma et al., 2015). In brief, mice were anesthetized with pentobarbital (50 mg/kg intraperitoneally) and underwent a laminectomy at the T11 and T12 level. After clamping the transverse processes of T11 and T12 to stabilize the spine, the exposed dorsal surface of the cord was subjected to a weight drop injury using a 10-g rod dropped from a height of 6.25 mm. After injury, the muscles and skin were closed in layers, and mice were placed in a temperature- and humidity-controlled chamber. Manual bladder emptying was performed three times daily until reflex bladder emptying was established.

### Bone marrow chimeras

Bone marrow chimeras were prepared as described previously (Gao et al., 2003). In brief, recipients were irradiated twice at 450 rad with a 2-h interval (total of 900 rad). Donor bone marrow cells were injected intravenously into recipients ( $10^7$  cells per mouse). Antibiotics were added to the drinking water for the first 4 wk after reconstitution. At 8 wk after reconstitution, the mice were used for SCI.

### Tissue processing

To harvest spinal cords, mice were deeply anesthetized with 1.25% tribromoethanol, and the blood was drawn off through cardiac puncture. A 10-mm segment of cord centered on T11 was removed and quickly frozen in an ethanol-dry ice bath. Samples were stored at  $-80^{\circ}\text{C}$ . The tissue samples were later homogenized in 200  $\mu\text{l}$  of ice-cold cell lysis buffer (Beyotime) containing enzyme inhibitors and centrifuged at 10,000  $\text{g}$  for 10 min at  $4^{\circ}\text{C}$ , and then the supernatants were frozen at  $-80^{\circ}\text{C}$ . Protein levels were determined with the bicinchoninic acid protein assay as described by the manufacturer (Beyotime).

### Immunohistochemistry

For immunofluorescence staining, spinal cord tissues were resected from mice 8 wk after surgery. Mice were deeply anesthetized with 1.25% tribromoethanol after thoracotomy, and 10 ml of normal saline was rapidly perfused through the left ventricle. This was followed by perfusion of 30 ml of 4% paraformaldehyde for fixation. A spinal cord segment measuring 5

mm in length was resected from the level of T11 and soaked in 4% paraformaldehyde for 24 h before being transferred into 30% sucrose solution until the tissue sank. After freezing, the tissues were cut into  $\sim$ 15–20- $\mu\text{m}$  sections (Leica). Slices were incubated with the following mouse-specific primary antibodies: 1:1,000 anti-GFAP (ab7260; Abcam), 1:200 anti-ChAT (AB144P; Millipore), 1:500 anti-SMI32 (NE1023; Merck), and 1:200 anti-iNOS (BD610328; Abcam). For visualization, 1:1,000 fluorescent Alexa Fluor 488 or 546 secondary antibodies (Invitrogen Vector) were used for both or single staining at room temperature for 2 h. After washing, the tissue slices were fixed with Vectashield containing DAPI and used for visualization. An inverted fluorescence microscope (Axio Observer A1; Carl Zeiss) was used to capture images and conduct further analysis. To determine the total number of neurons, the number of motor neurons in both spinal cord anterior horns was estimated.

### Image analysis

The densities of  $\gamma\delta^+$  cells and IFN- $\gamma^+$  cells were quantified and expressed as the numbers of marker $^+$  cells divided by the area of outlined regions. A 0.1-mm $^2$  area per image was selected randomly for quantification. Five slices per mouse and six mice per genotype were quantified.  $\gamma\delta^+$  cells and V $\gamma$ 1  $\gamma\delta^+$  or V $\gamma$ 4  $\gamma\delta^+$  cells were quantified and expressed as the numbers of marker $^+$  cells divided by a 0.1-mm $^2$  area per image. Five slices per mouse and six mice per genotype were quantified. Sections matched in anatomy were serially chosen (Fu et al., 2017).

For quantitative analysis of cavity volume, serial spinal cord sections stained with GFAP were three-dimensionally reconstructed. A total of five serial transverse spinal cord sections equally spaced 200  $\mu\text{m}$  apart were used to create a three-dimensional image corresponding to a 1-cm-long spinal cord segment. The lesion cavity and the spinal cord were three-dimensionally reconstructed with a microscope attached to a Neurolucida system (MBF Bioscience). The Neurolucida software calculated the volumes of the cystic cavities automatically (Gu et al., 2010).

### BMS

The BMS primary scoring system is based on a scale that ranges from 0 (complete paralysis) to 9 points (completely normal). The mice were placed on a flat surface and observed for 5 min. Hind limb motor functions were scored by the single-blind method using two independent blind observers. The mean score of both observers for two hind limbs was used as the BMS of the sample.

### EthoVision-assisted open-field test

Mice were placed under illumination (500 lx) in one corner of a 50  $\times$  50  $\times$  35-cm box. The trajectories of mice were recorded for 15 min. Five mice from each group were continuously monitored. A video-tracking system (XT 7.0 EthoVision; Noldus) was used to analyze trajectories and total movements.

### CatWalk-assisted gait analysis

Gait analysis of mice from each group was conducted using an automated quantitative gait analysis system (CatWalk XT; Noldus). Each mouse was subjected to at least three assessments, each of which required continuous walking on a glass plate, along a path that was 50 cm in length. The entire experiment was conducted in a dark, quiet environment. The CatWalk system automatically identified and tagged each paw print and then generated a series of parameters, including paw statistics, general parameters (mean speed and cadence), step sequence parameters, and bases of support. The walking coordination was assessed using the regularity index as described previously (Koopmans et al., 2005), calculated as the number of normal step sequence patterns multiplied by four and divided by the total amount of paw placements; that value is  $\sim 100\%$  in normal animals. The max contact area was indicated by the maximal area of contact between the paw and the walking floor.

### Sample collection from patients

Patients sustaining acute SCI were recruited at The First Affiliated Hospital of Jinan University by neurosurgeons from May 2013 to June 2017. Inclusion criteria for the trial included American Spinal Injury Association (ASIA) grade A or B SCI upon presentation, spinal injury between C4 and T10 inclusive, within 48 h after injury and the ability to provide a valid, reliable neurological examination. Patients were excluded if they had concomitant head injuries, concomitant major trauma to the chest, pelvis, or extremities that required invasive intervention (e.g., chest tube, internal or external fixation), or if they were too sedated or intoxicated to undergo a valid neurological examination. The CSF from SCI patients was obtained via myelotomy. To obtain the control samples from non-SCI patients, we enrolled individuals with hip osteoarthritis who were undergoing hip replacements under spinal anesthesia. The anesthesiologist punctured the dura with a spinal needle, and a 1.5–2.0-ml sample of CSF was collected, after which the anesthetic agent was injected (Kwon et al., 2010). The clinical trial protocol was approved by the Human Ethics Committee at Jinan University, and the sample collection was approved by individual patients.

### Cytokine analysis

The human CSF was analyzed on a Bio-Plex system (BioRad) using a 17-plex human cytokine kit that included IL-1 $\beta$ , IL-2, IL-4, IL-5, IL-6, IL-7, IL-8, IL-10, IL-12p40, IL-13, IL-17, MCP-1 (MCAF), IFN- $\gamma$ , GM-CSF, G-CSF, MIP-1 $\beta$ , and TNF- $\alpha$  (catalog no. M5000031YV). The mice spinal cords were analyzed with the Bio-Plex system using a 23-plex cytokine array kit that included Eotaxin, G-CSF, GM-CSF, IFN- $\gamma$ , IL-1 $\alpha$ , IL-1 $\beta$ , IL-2, IL-3, IL-4, IL-5, IL-6, IL-9, IL-10, IL-12 (p40), IL-12 (p70), IL-13, IL-17A, KC, MCP-1 (MCAF), MIP-1 $\alpha$ , MIP-1 $\beta$ , RANTES, and TNF- $\alpha$  (catalog no. M60009RDPD).

### Bone marrow isolation, differentiation, and polarization

Mouse bone marrow cells were flushed from the femur of WT or *IFN- $\gamma$ R1 $^{-/-}$*  mice (females, 8 wk old) and differentiated into BMDMs in DMEM with 10% FBS and 20 ng/ml M-CSF in a 6-well cell culture plate (10 $^6$  cells/ml) for 6 d (Zhang et al., 2008). BMDMs were also washed and resuspended in fresh media and incubated for a further 1 h in the presence of 100 ng/ml *Escherichia coli* 0111:B4 LPS (Sigma-Aldrich) and then were washed and proceeded to the cell lysis and protein extraction for Western blot testing.

### Western blot

BMDM lysates were obtained with radioimmunoprecipitation assay lysis buffer (50 mM Tris, pH 7.4, 150 mM NaCl, 1% Triton X-100, 1% sodium deoxycholate, 0.1% SDS, sodium orthovanadate, sodium fluoride, and EDTA; Beyotime), 2 mg/ml aprotinin, and 1 mM PMSF. Then they were subjected to 10,000 g centrifugation at 4°C for 20 min. The protein concentration was measured by a bicinchoninic acid protein assay kit. The immunoblotting was performed as described previously (Zhu et al., 2014; Zhao et al., 2017), and the following primary antibodies were used: anti-p65, p-p65 (Ser 468), p-p65 (Ser 536), STAT-1, p-STAT-1, and GAPDH, all from Cell Signaling Technology.

### $\gamma\delta$ T cell proliferation and transplantation

For expansion of V $\gamma$ 1, V $\gamma$ 4, and  $\gamma\delta$  T cells from WT or *IFN- $\gamma$ R1 $^{-/-}$*  mice in vitro, splenic  $\gamma\delta$  T cells were sorted and expanded with anti-V $\gamma$ 1 anti-V $\gamma$ 4 or anti- $\gamma\delta$  antibodies as described previously (Hao et al., 2011). For polarization of T cells, the cells were cultured with 10  $\mu$ g/ml of plate-coated anti-CD3, 1  $\mu$ g/ml of soluble anti-CD28, and 2 ng/ml IL-2 in the neutral culture medium as described previously (He et al., 2010; Zhao et al., 2011). In cell transfer experiments, PBS, V $\gamma$ 1, V $\gamma$ 4, or  $\gamma\delta$  T cells (10 $^6$  cells per mouse) from WT or *IFN- $\gamma$ R1 $^{-/-}$*  mice were transplanted into the *TCR $\delta$ R1 $^{-/-}$*  mice (10 mice per group) with intravenous injection. 1 d after the transplantation, all mice received contusive SCI, and ethology evaluation followed.

### Flow cytometry

Macrophages were put in a new well and treated with 1:1,000 GolgiPlug and 1 ng/ml ionomycin for 6 h and then were permeabilized with 0.5% (wt/vol) saponin for 30 min (37°C, 5% of CO<sub>2</sub>). The intracellular and cell surface staining were performed as the protocol described in the fixation/permeabilization kit (554714; BD). For cytokine staining, cells were collected and incubated with FITC anti-mouse TNF- $\alpha$  for 30 min at 4°C, washed with PBS, labeled with cell surface-staining marker PE-anti-mouse F4/80, APC-anti-mouse CD86, and PerCP-anti-mouse CD11c for 20 min at 4°C, and detected by FACS versus flow cytometry (BD). Data were analyzed using FlowJo (TreeStar).

### MEP recording

The MEPs were assayed by electromyography on the mice 8 wk after surgery as described previously (Ding et al., 2014),

with minor modifications. A stimulation electrode was applied to the rostral extremity of the surgically exposed spinal cord region, and the recording electrode was placed in the biceps flexor cruris. A single square wave stimulus of 0.5 mA, 0.5 ms in duration, 2-ms time delay, and 1 Hz was used. The latency period was measured as the length of time from the stimulus to the onset of the first response wave. The amplitude was measured from the initiation point of the first response wave to its highest point. The peak-to-peak amplitude (P-P value) was calculated to estimate the nerve conduction function in the hind limb.

### Statistical analysis

The SPSS 19.0 statistical software (IBM) was used to process and analyze the data and images. Data were presented as the mean  $\pm$  SEM. For analyzing the differences in BMSs between the groups over time, a two-way repeated measures ANOVA with Bonferroni's post-hoc correction was performed. Other data were analyzed using Student's *t* test or one-way ANOVA with Tukey's multiple comparison test. All tests were two sided, and the level of significance was set at 0.05.

### Online supplemental material

Fig. S1 contains data showing the validation of  $\gamma\delta$  T cell transfer, of  $\gamma\delta$  T cell depletion after antibody treatment, of *TCR- $\delta^{-/-}$*  mice, and of chimeric experiments and the infiltration of  $\gamma\delta$  T cells after SCI. Fig. S2 shows morphological changes in spinal cords of *TCR $\delta^{-/-}$*  mice reconstituted after SCI with  $\gamma\delta$  T cells from WT or *IFN- $\gamma^{-/-}$*  mice. Fig. S3 includes the results of CatWalk tests in WT mice reconstituted after SCI with different macrophages. Fig. S4 shows the levels of inflammatory cytokines in different mice 24 h after SCI, analyzed using the Bio-Plex system. Fig. S5 shows M2 macrophages present in the lesion site in *IFN- $\gamma R^{-/-}$*  mouse after SCI.

### ACKNOWLEDGMENTS

We wish to thank Hezuo Lü for technical support with animal models, Xin Sun, Panpan Yu and Yiwen Ruan for critical comments, and Andre M. Goffinet for revising the manuscript.

This work is supported by the National Natural Science Foundation of China (grant 31400770 to Z. Yin and grant 81571186 to L. Zhou), the 111 Project (grant B14036 to L. Zhou and grant B16021 to Z. Yin), the National Basic Research Program of China (973 Program; grant 2014CB542205 to L. Zhou), the Science & Technology Planning and Key Technology Innovation Projects of Guangdong (grant 2014B050504006 to L. Zhou), the Program for Changjiang Scholars and Innovative Research Team in University of Ministry of Education of China (grant IRT-15R13 to Y. Zhao), and the Guangdong Innovative and Entrepreneurial Research Program (grant 201301s0105240297 to Z. Yin).

The authors declare no competing financial interests.

Author contributions: Z. Yin, L. Zhou, and K.-F. So designed experiments; G. Sun, S. Yang, and G. Cao performed research; Q. Wang, J. Hao, Q. Wen, and Z. Liu assisted in animal models and data analysis; Z. Li, S. Zhou, and Y. Zhao contributed to study design; G. Sun, S. Yang, and H. Yang prepared the manuscript; Z. Yin and L. Zhou revised the manuscript.

Submitted: 13 April 2017

Revised: 22 August 2017

Accepted: 28 November 2017

### REFERENCES

Ankeny, D.P., and P.G. Popovich. 2009. Mechanisms and implications of adaptive immune responses after traumatic spinal cord injury. *Neuroscience*. 158:1112–1121. <https://doi.org/10.1016/j.neuroscience.2008.07.001>

Anwar, M.A., T.S. Al Shehabi, and A.H. Eid. 2016. Inflammogenesis of Secondary Spinal Cord Injury. *Front. Cell. Neurosci.* 10:98. <https://doi.org/10.3389/fncel.2016.00098>

Baskin, D.S., and R.K. Simpson Jr. 1987. Corticomotor and somatosensory evoked potential evaluation of acute spinal cord injury in the rat. *Neurosurgery*. 20:871–877. <https://doi.org/10.1227/00006123-198706000-00009>

Bayrakli, F., H. Balaban, U. Ozum, C. Duger, S. Topaktas, and H.Z. Kars. 2012. Etanercept treatment enhances clinical and neuroelectrophysiological recovery in partial spinal cord injury. *Eur. Spine J.* 21:2588–2593. <https://doi.org/10.1007/s00586-012-2319-7>

Becher, B., S. Spath, and J. Goverman. 2017. Cytokine networks in neuroinflammation. *Nat. Rev. Immunol.* 17:49–59. <https://doi.org/10.1038/nri.2016.123>

Beg, A.A., and D. Baltimore. 1996. An essential role for NF-kappaB in preventing TNF-alpha-induced cell death. *Science*. 274:782–784. <https://doi.org/10.1126/science.274.5288.782>

Beg, A.A., T.S. Finco, P.V. Nantermet, and A.S. Baldwin Jr. 1993. Tumor necrosis factor and interleukin-1 lead to phosphorylation and loss of I kappa B alpha: a mechanism for NF-kappa B activation. *Mol. Cell. Biol.* 13:3301–3310. <https://doi.org/10.1128/MCB.13.6.3301>

Benakis, C., D. Brea, S. Caballero, G. Faraco, J. Moore, M. Murphy, G. Sita, G. Racchumi, L. Ling, E.G. Pamer, et al. 2016. Commensal microbiota affects ischemic stroke outcome by regulating intestinal  $\gamma\delta$  T cells. *Nat. Med.* 22:516–523. <https://doi.org/10.1038/nm.4068>

Bonneville, M., R.L. O'Brien, and W.K. Born. 2010. Gammadelta T cell effector functions: a blend of innate programming and acquired plasticity. *Nat. Rev. Immunol.* 10:467–478. <https://doi.org/10.1038/nri2781>

Ceccarelli, F., U. Massafra, C. Perricone, L. Idolazzi, R. Giacomelli, R. Tirri, R. Russo, G. Pistone, P. Ruscitti, S. Parisi, et al. 2017. Anti-TNF treatment response in rheumatoid arthritis patients with moderate disease activity: a prospective observational multicentre study (MODERATE). *Clin. Exp. Rheumatol.* 35:24–32.

Chen, L., W. He, S.T. Kim, J. Tao, Y. Gao, H. Chi, A.M. Intlekofer, B. Harvey, S.L. Reiner, Z. Yin, et al. 2007. Epigenetic and transcriptional programs lead to default IFN-gamma production by gammadelta T cells. *J. Immunol.* 178:2730–2736. <https://doi.org/10.4049/jimmunol.178.5.2730>

Cusimano, M., D. Biziato, E. Brambilla, M. Donegà, C. Alfaro-Cervello, S. Snider, G. Salani, F. Pucci, G. Comi, J.M. Garcia-Verdugo, et al. 2012. Transplanted neural stem/precursor cells instruct phagocytes and reduce secondary tissue damage in the injured spinal cord. *Brain*. 135:447–460. <https://doi.org/10.1093/brain/awr339>

Daley, D., C.P. Zambirinis, L. Seifert, N. Akkad, N. Mohan, G. Werba, R. Barilla, A. Torres-Hernandez, M. Hundeyin, V.R.K. Mani, et al. 2016.  $\gamma\delta$  T Cells Support Pancreatic Oncogenesis by Restraining  $\alpha\beta$  T Cell Activation. *Cell*. 166:1485–1499.e15. <https://doi.org/10.1016/j.cell.2016.07.046>

David, S., and A. Krone. 2011. Repertoire of microglial and macrophage responses after spinal cord injury. *Nat. Rev. Neurosci.* 12:388–399. <https://doi.org/10.1038/nrn3053>

Ding, Y., Y. Qu, J. Feng, M. Wang, Q. Han, K.F. So, W. Wu, and L. Zhou. 2014. Functional motor recovery from motoneuron axotomy is compromised in mice with defective corticospinal projections. *PLoS One*. 9:e101918. <https://doi.org/10.1371/journal.pone.0101918>

Fu, Q., M.M. Zou, J.W. Zhu, Y. Zhang, W.J. Chen, M. Cheng, C.F. Liu, Q.H. Ma, and R.X. Xu. 2017. TRIM32 affects the recovery of motor function following spinal cord injury through regulating proliferation of glia. *Oncotarget*. 8:45380–45390. <https://doi.org/10.18632/oncotarget.17492>

Fujiyoshi, T., T. Kubo, C.C. Chan, M. Koda, A. Okawa, K. Takahashi, and M. Yamazaki. 2010. Interferon- $\gamma$  decreases chondroitin sulfate proteoglycan

expression and enhances hindlimb function after spinal cord injury in mice. *J. Neurotrauma.* 27:2283–2294. <https://doi.org/10.1089/neu.2009.1144>

Gao, Y., W. Yang, M. Pan, E. Scully, M. Girardi, L.H. Augenlicht, J. Craft, and Z. Yin. 2003.  $\gamma\delta$  T cells provide an early source of interferon gamma in tumor immunity. *J. Exp. Med.* 198:433–442. <https://doi.org/10.1084/jem.20030584>

Genovese, T., E. Mazzon, C. Crisafulli, R. Di Paola, C. Muià, P. Bramanti, and S. Cuzzocrea. 2006. Immunomodulatory effects of etanercept in an experimental model of spinal cord injury. *J. Pharmacol. Exp. Ther.* 316:1006–1016. <https://doi.org/10.1124/jpet.105.097188>

Genovese, T., E. Mazzon, C. Crisafulli, E. Esposito, R. Di Paola, C. Muià, P. Di Bella, R. Meli, P. Bramanti, and S. Cuzzocrea. 2007. Combination of dexamethasone and etanercept reduces secondary damage in experimental spinal cord trauma. *Neuroscience.* 150:168–181. <https://doi.org/10.1016/j.neuroscience.2007.06.059>

Gordon, S., and P.R. Taylor. 2005. Monocyte and macrophage heterogeneity. *Nat. Rev. Immunol.* 5:953–964. <https://doi.org/10.1038/nri1733>

Gu, W., F. Zhang, Q. Xue, Z. Ma, P. Lu, and B. Yu. 2010. Transplantation of bone marrow mesenchymal stem cells reduces lesion volume and induces axonal regrowth of injured spinal cord. *Neuropathology.* 30:205–217. <https://doi.org/10.1111/j.1440-1789.2009.01063.x>

Hahn, Y.-S., C. Taube, N. Jin, L. Sharp, J.M. Wands, M.K. Aydintug, M. Lahn, S.A. Huber, R.L. O'Brien, E.W. Gelfand, and W.K. Born. 2004. Different potentials of gamma delta T cell subsets in regulating airway responsiveness: V gamma 1+ cells, but not V gamma 4+ cells, promote airway hyperreactivity, Th2 cytokines, and airway inflammation. *J. Immunol.* 172:2894–2902. <https://doi.org/10.4049/jimmunol.172.5.2894>

Hao, J., S. Dong, S. Xia, W. He, H. Jia, S. Zhang, J. Wei, R.L. O'Brien, W.K. Born, Z. Wu, et al. 2011. Regulatory role of V $\gamma$ 1  $\gamma\delta$  T cells in tumor immunity through IL-4 production. *J. Immunol.* 187:4979–4986. <https://doi.org/10.4049/jimmunol.1101389>

He, W., J. Hao, S. Dong, Y. Gao, J. Tao, H. Chi, R. Flavell, R.L. O'Brien, W.K. Born, J. Craft, et al. 2010. Naturally activated V $\gamma$ 4  $\gamma\delta$  T cells play a protective role in tumor immunity through expression of eomesodermin. *J. Immunol.* 185:126–133. <https://doi.org/10.4049/jimmunol.0903767>

Heilig, J.S., and S. Tonegawa. 1986. Diversity of murine gamma genes and expression in fetal and adult T lymphocytes. *Nature.* 322:836–840. <https://doi.org/10.1038/322836a0>

Holderness, J., J.F. Hedges, A. Ramstead, and M.A. Jutila. 2013. Comparative biology of  $\gamma\delta$  T cell function in humans, mice, and domestic animals. *Annu. Rev. Anim. Biosci.* 1:99–124. <https://doi.org/10.1146/annurev-animal-031412-103639>

Huang, Y., N. Jin, C.L. Roark, M.K. Aydintug, J.M. Wands, H. Huang, R.L. O'Brien, and W.K. Born. 2009. The influence of IgE-enhancing and IgE-suppressive gammadelta T cells changes with exposure to inhaled ovalbumin. *J. Immunol.* 183:849–855. <https://doi.org/10.4049/jimmunol.0804104>

Huber, S.A., D. Graveline, M.K. Newell, W.K. Born, and R.L. O'Brien. 2000. V $\gamma$ 1+ T cells suppress and V $\gamma$ 4+ T cells promote susceptibility to coxsackievirus B3-induced myocarditis in mice. *J. Immunol.* 165:4174–4181. <https://doi.org/10.4049/jimmunol.165.8.4174>

Ishii, H., S. Tanabe, M. Ueno, T. Kubo, H. Kayama, S. Serada, M. Fujimoto, K. Takeda, T. Naka, and T. Yamashita. 2013. Ifn- $\gamma$ -dependent secretion of IL-10 from Th1 cells and microglia/macrophages contributes to functional recovery after spinal cord injury. *Cell Death Dis.* 4:e710. <https://doi.org/10.1038/cddis.2013.234>

Ito, K., M. Bonneville, Y. Takagaki, N. Nakanishi, O. Kanagawa, E.G. Krecko, and S. Tonegawa. 1989. Different gamma delta T-cell receptors are expressed on thymocytes at different stages of development. *Proc. Natl. Acad. Sci. USA.* 86:631–635. <https://doi.org/10.1073/pnas.86.2.631>

Itohara, S., P. Mombaerts, J. Lafaille, J. Iacomini, A. Nelson, A.R. Clarke, M.L. Hooper, A. Farr, and S. Tonegawa. 1993. T cell receptor delta gene mutant mice: independent generation of alpha beta T cells and programmed rearrangements of gamma delta TCR genes. *Cell.* 72:337–348. [https://doi.org/10.1016/0092-8674\(93\)90112-4](https://doi.org/10.1016/0092-8674(93)90112-4)

Jensen, K.D., X. Su, S. Shin, L. Li, S. Youssef, S. Yamasaki, L. Steinman, T. Saito, R.M. Locksley, M.M. Davis, et al. 2008. Thymic selection determines gammadelta T cell effector fate: antigen-naive cells make interleukin-17 and antigen-experienced cells make interferon gamma. *Immunity.* 29:90–100. <https://doi.org/10.1016/j.jimmuni.2008.04.022>

Kemény-Beke, A., Z. Szekanecz, S. Szántó, N. Bodnár, L. Módis Jr., R. Gesztesy, J. Zsuga, P. Szodoray, and A. Berta. 2010. Safety and efficacy of etanercept therapy in ankylosing spondylitis patients undergoing phacoemulsification surgery. *Rheumatology (Oxford).* 49:2220–2221. <https://doi.org/10.1093/rheumatology/keq288>

Kigerl, K.A., J.C. Gensel, D.P. Ankeny, J.K. Alexander, D.J. Donnelly, and P.G. Popovich. 2009. Identification of two distinct macrophage subsets with divergent effects causing either neurotoxicity or regeneration in the injured mouse spinal cord. *J. Neurosci.* 29:13435–13444. <https://doi.org/10.1523/JNEUROSCI.3257-09.2009>

Kleine, T.O., P. Zwerenz, P. Zöfel, and K. Shiratori. 2003. New and old diagnostic markers of meningitis in cerebrospinal fluid (CSF). *Brain Res. Bull.* 61:287–297. [https://doi.org/10.1016/S0361-9230\(03\)00092-3](https://doi.org/10.1016/S0361-9230(03)00092-3)

Koenecke, C., V. Chennupati, S. Schmitz, B. Malissen, R. Förster, and I. Prinz. 2009. In vivo application of mAb directed against the gammadelta TCR does not deplete but generates “invisible” gammadelta T cells. *Eur. J. Immunol.* 39:372–379. <https://doi.org/10.1002/eji.200838741>

Koopmans, G.C., R. Deumens, W.M. Honig, F.P. Hamers, H.W. Steinbusch, and E.A. Joosten. 2005. The assessment of locomotor function in spinal cord injured rats: the importance of objective analysis of coordination. *J. Neurotrauma.* 22:214–225. <https://doi.org/10.1089/neu.2005.22.214>

Kwon, B.K., A.M. Stammers, L.M. Belanger, A. Bernardo, D. Chan, C.M. Bishop, G.P. Slobogean, H. Zhang, H. Umedaly, M. Giffin, et al. 2010. Cerebrospinal fluid inflammatory cytokines and biomarkers of injury severity in acute human spinal cord injury. *J. Neurotrauma.* 27:669–682. <https://doi.org/10.1089/neu.2009.1080>

Lech, M., and H.J. Anders. 2013. Macrophages and fibrosis: How resident and infiltrating mononuclear phagocytes orchestrate all phases of tissue injury and repair. *Biochim. Biophys. Acta.* 1832:989–997. <https://doi.org/10.1016/j.bbadi.2012.12.001>

Liebermann, T.A., and D. Baltimore. 1990. Activation of interleukin-6 gene expression through the NF-kappa B transcription factor. *Mol. Cell. Biol.* 10:2327–2334. <https://doi.org/10.1128/MCB.10.5.2327>

Luan, H., Q. Zhang, L. Wang, C. Wang, M. Zhang, X. Xu, H. Zhou, X. Li, Q. Xu, F. He, et al. 2014. OM85-BV induced the productions of IL-1 $\beta$ , IL-6, and TNF- $\alpha$  via TLR4- and TLR2-mediated ERK1/2/NF- $\kappa$ B pathway in RAW264.7 cells. *J. Interferon Cytokine Res.* 34:526–536. <https://doi.org/10.1089/jir.2013.0077>

Ma, S.F., Y.J. Chen, J.X. Zhang, L. Shen, R. Wang, J.S. Zhou, J.G. Hu, and H.Z. Lü. 2015. Adoptive transfer of M2 macrophages promotes locomotor recovery in adult rats after spinal cord injury. *Brain Behav. Immun.* 45:157–170. <https://doi.org/10.1016/j.bbi.2014.11.007>

Malik, S., M.Y. Want, and A. Awasthi. 2016. The Emerging Roles of Gamma-Delta T Cells in Tissue Inflammation in Experimental Autoimmune Encephalomyelitis. *Front. Immunol.* 7:14. <https://doi.org/10.3389/fimmu.2016.00014>

Marchand, F., C. Tsantoulas, D. Singh, J. Grist, A.K. Clark, E.J. Bradbury, and S.B. McMahon. 2009. Effects of Etanercept and Minocycline in a rat model of spinal cord injury. *Eur. J. Pain.* 13:673–681. <https://doi.org/10.1016/j.ejpain.2008.08.001>

Mattson, M.P., and S. Camandola. 2001. NF-kappaB in neuronal plasticity and neurodegenerative disorders. *J. Clin. Invest.* 107:247–254. <https://doi.org/10.1172/JCI11916>

Mozaffari, S., S. Nikfar, A.H. Abdolghaffari, and M. Abdollahi. 2014. New biologic therapeutics for ulcerative colitis and Crohn's disease. *Expert*

*Opin. Biol. Ther.* 14:583–600. <https://doi.org/10.1517/14712598.2014.885945>

Murray, P.J., J.E. Allen, S.K. Biswas, E.A. Fisher, D.W. Gilroy, S. Goerdt, S. Gordon, J.A. Hamilton, L.B. Ivashkiv, T. Lawrence, et al. 2014. Macrophage activation and polarization: nomenclature and experimental guidelines. *Immunity*. 41:14–20. <https://doi.org/10.1016/j.jimmuni.2014.06.008>

Olmos, G., and J. Lladó. 2014. Tumor necrosis factor alpha: a link between neuroinflammation and excitotoxicity. *Mediators Inflamm.* 2014:861231. <https://doi.org/10.1155/2014/861231>

Ottum, P.A., G. Arellano, L.I. Reyes, M. Iruretagoyena, and R. Naves. 2015. Opposing Roles of Interferon-Gamma on Cells of the Central Nervous System in Autoimmune Neuroinflammation. *Front. Immunol.* 6:539. <https://doi.org/10.3389/fimmu.2015.00539>

Papoutsaki, M., and A. Costanzo. 2013. Treatment of psoriasis and psoriatic arthritis. *BioDrugs.* 27(S1, Suppl 1):3–12. <https://doi.org/10.1007/BF03325637>

Pereira, P., D. Gerber, S.Y. Huang, and S. Tonegawa. 1995. Ontogenetic development and tissue distribution of V gamma 1-expressing gamma/delta T lymphocytes in normal mice. *J. Exp. Med.* 182:1921–1930. <https://doi.org/10.1084/jem.182.6.1921>

Pitt, D., P. Werner, and C.S. Raine. 2000. Glutamate excitotoxicity in a model of multiple sclerosis. *Nat. Med.* 6:67–70. <https://doi.org/10.1038/71555>

Prescott, K., M. Costner, S. Cohen, and S. Kazi. 2007. Tumor necrosis factor-alpha inhibitor associated ulcerative colitis. *Am. J. Med. Sci.* 333:137–139. <https://doi.org/10.1097/MAJ.0b013e3180312362>

Prieur, X., C.Y. Mok, V.R. Velagapudi, V. Núñez, L. Fuentes, D. Montaner, K. Ishikawa, A. Camacho, N. Barroja, S. O’Rahilly, et al. 2011. Differential lipid partitioning between adipocytes and tissue macrophages modulates macrophage lipotoxicity and M2/M1 polarization in obese mice. *Diabetes*. 60:797–809. <https://doi.org/10.2337/db10-0705>

Prinz, I., A. Sansoni, A. Kisselkell, L. Ardouin, M. Malissen, and B. Malissen. 2006. Visualization of the earliest steps of gammadelta T cell development in the adult thymus. *Nat. Immunol.* 7:995–1003. <https://doi.org/10.1038/ni1371>

Prinz, I., B. Silva-Santos, and D.J. Pennington. 2013. Functional development of  $\gamma\delta$  T cells. *Eur. J. Immunol.* 43:1988–1994. <https://doi.org/10.1002/eji.201343759>

Ramer, L.M., M.S. Ramer, and E.J. Bradbury. 2014. Restoring function after spinal cord injury: towards clinical translation of experimental strategies. *Lancet Neurol.* 13:1241–1256. [https://doi.org/10.1016/S1474-4422\(14\)70144-9](https://doi.org/10.1016/S1474-4422(14)70144-9)

Rayen, J., T. Currie, R.B. Garry, F. Frizelle, and T. Eglinton. 2017. The long-term outcome of anti-TNF alpha therapy in perianal Crohn’s disease. *Tech. Coloproctol.* 21:119–124. <https://doi.org/10.1007/s10151-016-1578-4>

Rubiano, A.M., N. Carney, R. Chesnut, and J.C. Puyana. 2015. Global neurotrauma research challenges and opportunities. *Nature*. 527:S193–S197. <https://doi.org/10.1038/nature16035>

Schmolka, N., M. Wencker, A.C. Hayday, and B. Silva-Santos. 2015. Epigenetic and transcriptional regulation of  $\gamma\delta$  T cell differentiation: Programming cells for responses in time and space. *Semin. Immunol.* 27:19–25. <https://doi.org/10.1016/j.smim.2015.01.001>

Schnell, L., S. Fearn, H. Klassen, M.E. Schwab, and V.H. Perry. 1999. Acute inflammatory responses to mechanical lesions in the CNS: differences between brain and spinal cord. *Eur. J. Neurosci.* 11:3648–3658. <https://doi.org/10.1046/j.1460-9568.1999.00792.x>

Shichita, T., Y. Sugiyama, H. Ooboshi, H. Sugimori, R. Nakagawa, I. Takada, T. Iwaki, Y. Okada, M. Iida, D.J. Cua, et al. 2009. Pivotal role of cerebral interleukin-17-producing gammadeltaT cells in the delayed phase of ischemic brain injury. *Nat. Med.* 15:946–950. <https://doi.org/10.1038/nm.1999>

Silver, J., M.E. Schwab, and P.G. Popovich. 2015. Central nervous system regenerative failure: role of oligodendrocytes, astrocytes, and microglia. *Cold Spring Harb. Perspect. Biol.* 7:a020602. <https://doi.org/10.1101/cshperspect.a020602>

Skeen, M.J., E.P. Rix, M.M. Freeman, and H.K. Ziegler. 2001. Exaggerated proinflammatory and Th1 responses in the absence of gamma/delta T cells after infection with Listeria monocytogenes. *Infect. Immun.* 69:7213–7223. <https://doi.org/10.1128/IAI.69.12.7213-7223.2001>

Smith, J.A., R. Zhang, A.K. Varma, A. Das, S.K. Ray, and N.L. Banik. 2009. Estrogen partially down-regulates PTEN to prevent apoptosis in VSC4.1 motoneurons following exposure to IFN-gamma. *Brain Res.* 1301:163–170. <https://doi.org/10.1016/j.brainres.2009.09.016>

Sumitomo, M., M. Tachibana, J. Nakashima, M. Murai, A. Miyajima, F. Kimura, M. Hayakawa, and H. Nakamura. 1999. An essential role for nuclear factor kappa B in preventing TNF-alpha-induced cell death in prostate cancer cells. *J. Urol.* 161:674–679. [https://doi.org/10.1016/S0022-5347\(01\)61993-1](https://doi.org/10.1016/S0022-5347(01)61993-1)

Ung, R.V., N.P. Lapointe, C. Tremblay, A. Larouche, and P.A. Guertin. 2007. Spontaneous recovery of hindlimb movement in completely spinal cord transected mice: a comparison of assessment methods and conditions. *Spinal Cord.* 45:367–379. <https://doi.org/10.1038/sj.sc.3101970>

Victório, S.C., L.P. Cartarozzi, R.C. Hell, and A.L. Oliveira. 2012. Decreased MHC I expression in IFN  $\gamma$  mutant mice alters synaptic elimination in the spinal cord after peripheral injury. *J. Neuroinflammation*. 9:88. <https://doi.org/10.1186/1742-2094-9-88>

Wang, X., K. Cao, X. Sun, Y. Chen, Z. Duan, L. Sun, L. Guo, P. Bai, D. Sun, J. Fan, et al. 2015. Macrophages in spinal cord injury: phenotypic and functional change from exposure to myelin debris. *Glia*. 63:635–651. <https://doi.org/10.1002/glia.22774>

Wu, D., P. Wu, F. Qiu, Q. Wei, and J. Huang. 2017. Human  $\gamma\delta$ T-cell subsets and their involvement in tumor immunity. *Cell. Mol. Immunol.* 14:245–253. <https://doi.org/10.1038/cmi.2016.55>

Yu, X.-J., D.-M. Zhang, L.-L. Jia, J. Qi, X.-A. Song, H. Tan, W. Cui, W. Chen, G.-Q. Zhu, D.-N. Qin, and Y.M. Kang. 2015. Inhibition of NF- $\kappa$ B activity in the hypothalamic paraventricular nucleus attenuates hypertension and cardiac hypertrophy by modulating cytokines and attenuating oxidative stress. *Toxicol. Appl. Pharmacol.* 284:315–322. <https://doi.org/10.1016/j.taap.2015.02.023>

Zhang, X., R. Goncalves, and D.M. Mosser. 2008. The isolation and characterization of murine macrophages. *Curr. Protoc. Immunol.* <https://doi.org/10.1002/0471142735.im1401s83>

Zhao, N., J. Hao, Y. Ni, W. Luo, R. Liang, G. Cao, Y. Zhao, P. Wang, L. Zhao, Z. Tian, et al. 2011. V $\gamma$ 4  $\gamma\delta$  T cell-derived IL-17A negatively regulates NKT cell function in Con A-induced fulminant hepatitis. *J. Immunol.* 187:5007–5014. <https://doi.org/10.4049/jimmunol.1101315>

Zhao, R., Y. Liu, H. Wang, J. Yang, W. Niu, S. Fan, W. Xiong, J. Ma, X. Li, J.B. Phillips, et al. 2017. BRD7 plays an anti-inflammatory role during early acute inflammation by inhibiting activation of the NF- $\kappa$ B signaling pathway. *Cell. Mol. Immunol.* 14:830–841. <https://doi.org/10.1038/cmi.2016.31>

Zhu, E., X. Wang, B. Zheng, Q. Wang, J. Hao, S. Chen, Q. Zhao, L. Zhao, Z. Wu, and Z. Yin. 2014. miR-20b suppresses Th17 differentiation and the pathogenesis of experimental autoimmune encephalomyelitis by targeting ROR $\gamma$ t and STAT3. *J. Immunol.* 192:5599–5609. <https://doi.org/10.4049/jimmunol.1303488>